UNIVERSIDADE ESTADUAL PAULISTA

FACULDADE DE CIÊNCIAS AGRÁRIAS E VETERINÁRIAS

CAMPUS DE JABOTICABAL

MODELOS AGROMETEOROLÓGICOS PARA TOMADORES DE DECISÃO EM 'SMART AGRICULTURE'

Taynara Tuany Borges Valeriano

Engenheira Agrônoma Ma. Agronomia (Produção Vegetal)

2019

UNIVERSIDADE ESTADUAL PAULISTA

FACULDADE DE CIÊNCIAS AGRÁRIAS E VETERINÁRIAS

CAMPUS DE JABOTICABAL

MODELOS AGROMETEOROLÓGICOS PARA TOMADORES DE DECISÃO EM 'SMART AGRICULTURE'

Discente: Taynara Tuany Borges Valeriano

Orientador: Prof. Dr. Glauco de Souza Rolim

Tese apresentada à Faculdade de Ciências Agrárias e Veterinárias – Unesp, Campus de Jaboticabal, como parte das exigências para obtenção do título Doutora em Agronomia (Produção Vegetal).

2019

Ficha catalográfica

V163m

Valeriano, Taynara Tuany Borges
Modelos agrometeorológicos para tomadores de decisão em "Smart Agriculture" / Taynara Tuany Borges Valeriano. -- Jaboticabal, 2019
79 p.

Tese (doutorado) - Universidade Estadual Paulista (Unesp), Faculdade de Ciências Agrárias e Veterinárias, Jaboticabal
Orientador: Glauco de Souza Rolim

1. Agronomia. 2. Modelagem de informações. 3. Fitopatologia. 4. Doenças fúngicas. 5. Irrigação agrícolas. I. Título.

Sistema de geração automática de fichas catalográficas da Unesp. Biblioteca da Faculdade de Ciências Agrárias e Veterinárias, Jaboticabal. Dados fornecidos pelo autor(a).

UNIVERSIDADE ESTADUAL PAULISTA

Câmpus de Jaboticabal

CERTIFICADO DE APROVAÇÃO

TÍTULO DA TESE: MODELOS AGROMETEOROLÓGICOS PARA TOMADORES DE DECISÃO EM 'SMART AGRICULTURE'

AUTORA: TAYNARA TUANY BORGES VALERIANO
ORIENTADOR: GLAUCO DE SOUZA ROLIM

Aprovada como parte das exigências para obtenção do Título de Doutora em AGRONOMIA (PRODUÇÃO VEGETAL), pela Comissão Examinadora:

Prof. Dr. GLAUCO DE SOUZA ROLIM
Departamento de Ciências Exatas / FCAV / UNESP - Jaboticabal

Dra. GISÈLE MARIA FANTIN
Laboratório de Fitopatologia / Instituto Biológico - Campinas /SP

Prof. Dr. SILVIO APARECIDO LOPES
Fundo de Defesa da Citricultura / FUNDECITRUS - Araraquara/SP

Prof.Dr. JOSÉ EDUARDO BOFFINO DE ALMEIDA MONTEIRO (Videoconferência)
Embrapa Informática Agropecuária / Campinas / SP

Prof. Dr. ALAN RODRIGO PANOSSO
Departamento de Ciências Exatas / FCAV-UNESP/Jaboticabal-SP

Jaboticabal, 16 de maio de 2019

DADOS CURRICULARES DO AUTORA

Taynara Tuany Borges Valeriano, nascida em 04 de julho de 1991 no município Araxá, Estado de Minas Gerais. Ingressou no curso de Engenharia Agronômica no Instituto Federal de Educação, Ciência e Tecnologia do Triângulo Mineiro, Campus Uberaba, em março de 2010. No mesmo campus, foi bolsista do Programa de Educação Tutorial (PET) durante a gestão 2011-2014. Em fevereiro de 2015 obteve o título de Engenheira Agrônoma. Iniciou o curso de mestrado no Campus de Jaboticabal, em agosto de 2015 onde em fevereiro de 2017 obteve o título de mestra em Agronomia (Produção Vegetal). Em março de 2017 ingressou no programa de doutorado em Agronomia (Produção Vegetal) do Campus de Jaboticabal, onde aproximadamente dois anos depois, defende sua tese para obtenção do título de doutora em Agronomia (Produção Vegetal). Durante o período de doutoramento desenvolveu a pesquisa em parceria com o Conselho de pesquisa em agricultura e análise da economia agraria – Centro de Pesquisa em Agricultura e Ambiente (CREA-AA) em Bologna – Itália, onde residiu entre setembro de 2018 a fevereiro 2019 como bolsista da fundação de Coordenação de Aperfeiçoamento de Nível Superior (CAPES). Ao longo de sua trajetória acadêmica seguiu as linhas de pesquisa em agrometeorologia e modelagem de cultivos agrícolas; formou parcerias com empresas privadas e órgãos públicos para o desenvolvimento de trabalhos com objetivo de atender necessidades da sociedade na busca de novas tecnologias para agricultura e o agronegócio brasileiro.

“A mente que se abre a uma nova ideia jamais voltará ao seu tamanho original”.

Albert Einsten

A minha mãe Magna Regina Borges que me criou com todo o amor, carinho e educação que se pode dar a um filho e sacrificou-se para que eu realizasse meu sonho.

A senhora**, DEDICO!**

A minha família, **OFEREÇO**!

AGRADECIMENTOS

Em primeiro lugar agradeço a Deus por ter sempre me amparado nas minhas escolhas para que não me arrependesse e nem desistisse delas, por mais difíceis que fossem.

À Universidade Estadual Paulista "Júlio de Mesquita Filho", Faculdade de Ciências Agrárias e Veterinárias, Campus de Jaboticabal, em especial ao Programa de Pós-Graduação em Agronomia (Produção Vegetal) e ao Conselho Nacional de Desenvolvimento Científico e Tecnológico (CNPQ), pela concessão de bolsa (processo 141291/2017-6) e oportunidade de realizar um curso de pós-graduação.

Ao meu orientador Prof. Dr. Glauco de Souza Rolim que tenho uma admiração e consideração imensa pelo seu trabalho, bem como pela referência que é para todos nós, orientandos. Muito obrigado pelos ensinamentos passados, pela confiança em mim depositada e pelo laço de amizade criado.

O presente trabalho foi realizado com apoio da Coordenação de Aperfeiçoamento de Pessoal de Nível Superior - Brasil (CAPES) - Código de Financiamento 001.

Ao Consiglio per la Ricerca in Agricoltura e L'analisi dell' Economia Agraria (CREA) – Bologna, Itália, em especial ao diretor Dr. Marcello Donatelli, por ter me aceitado prontamente para a realização do doutorado sanduíche, por ter me recebido calorosamente e por ter oferecido todo o suporte para a realização da minha tese.

Ao meu coorientador do doutorado sanduíche Dr. Simone Bregaglio que tenho uma admiração e consideração imensa pelo seu trabalho. Muito obrigada por toda a confiança em mim depositada e paciência dedicada. Foram seis meses de muito aprendizado.

À toda minha família em especial minha mãe, Regina, minha irmã Gabriella, minha avó Anacleta (*in memorian*), minha tia Rita, meus padrinhos Luiz e Joana, meus primos João Antônio e Juliana, meu padrasto Neirimar, meus afilhados, Luís Guilherme, Isadora e Adrian Lucas, minha afilhada de coração Estela e meu tio Lázaro, pela paciência e pela ausência em suas vidas, durante todos esses anos de estudos até aqui. Obrigado por vocês acreditarem em mim!

À minha tia Márcia que sempre foi minha referência e me inspirou a seguir o caminho de professora. Muito obrigada por todo suporte, apoio e dedicação.

À minha prima Stefany Souza, pela cumplicidade, lealdade, carinho e amizade de todos esses anos.

As minhas irmãs de coração, Rayeny Ávila, Sayeny Ávila e Kárita Almeida as quais sempre estiveram ao meu lado me apoiando e incentivando.

À minha família de Jaboticabal, Adão, Edgard, Larissa, Everton, Albertina, Mailson, Letícia, Luan e Karol, que fizeram meus dias mais felizes e preencheram todos os meus almoços de domingo amenizando a saudade de casa.

Aos meus amigos e parceiros do GAS e do departamento de Ciências Exatas, José Reinaldo, Victor Moreto, Lucas Aparecido, Kamila Menezes, Aline, Valter, Nayanni, Lígia, Mary Jane, Paulo, Gustavo, Fernando, Bruna, Ludhanna, Gabriela, Thiago, Maria Elisa, Mara. Obrigada pela convivência e troca de experiência durante esse tempo, vocês fizeram do departamento de exatas o melhor da UNESP.

Aos amigos de longa data, Isabela, Ana Cristhina, Cristina, que, mesmo de longe torceram por mim e entenderam minha ausência.

Ao Emmanuel Moreira, por todo amparo e carinho.

Aos membros da banca da defesa, Prof. Dr. Alan Panosso, Dr. Gisele Fantin, Dr. Eduardo Monteiro e Dr. Silvio Lopes, que muito contribuíram para a Tese.

Aos colegas do Departamento de Ciências Exatas, Zezé, Shirlei, Adriana, Prof. Peruzzi, Prof. Newton, Carlão e Vanessa, muito obrigada pela convivência durante esse tempo.

Aos amigos que ganhei durante o doutorado Sanduíche, Ana Claudia Azevedo, Ana Claudia, Vinícius, Henrique e Emanoele, vocês foram fundamentais para a minha adaptação em Bologna.

A todos que de alguma forma contribuíram para que chegasse hoje aqui, o meu muito obrigada!

SUMÁRIO

MODELOS AGROMETEOROLÓGICOS PARA TOMADORES DE DECISÃO EM 'SMART AGRICULTURE'

RESUMO - A agricultura no mundo caminha em alta velocidade para a próxima revolução verde, a chamada revolução da agricultura digital, que combina outras grandes áreas que revolucionaram a agricultura, como as técnicas de biotecnologia e agricultura de precisão. Estas técnicas foram essenciais para aumento da produtividade agrícola no mundo. Agora, a agricultura digital pode otimizar ainda mais a associação dos dados climáticos no planejamento de safras e no manejo de cultivos agrícolas. O conceito "Smart Agriculture" está inserido no universo da agricultura digital como uma linha promissora e necessária para o futuro sustentável da agricultura. Este trabalho apresenta estratégias de manejo para áreas produtoras de cana-de-açúcar, como (i) um sistema de modelo mecanístico para a previsão da susceptibilidade da doença fúngica, ferrugem alaranjada, baseado nas condições meteorológicas; (ii) estimativa da infestação de *Mahanarva fimbriolata* por meio de Redes Neurais Artificiais; (iii) um aplicativo de smartphone para estimar a evapotranspiração potencial utilizando dados meteorológicos em grid, provenientes do sistema NASA-POWER. As estratégias propostas neste trabalho mostraram-se eficientes e promissoras para aplicação prática. O modelo de ferrugem alaranjada simulou com acurácia o índice de severidade de ferrugem alaranjada, e proporcionou a expansão das simulações, com o objetivo de verificar a susceptibilidade da ocorrência da doença em grandes áreas produtoras de cana-de-açúcar, como Brasil, Índia e Austrália. A utilização de redes neurais artificiais para estimar níveis de infestação de *Mahanarva fimbriolata*, se mostrou como uma alternativa viável e promissora. A estimativa da evapotranspiração potencial, utilizando dados meteorológicos em grid provenientes da NASA-POWER, obteve resultados com alta acurácia e precisão, tornando assim, o aplicativo de smartphone desenvolvido uma ferramenta no auxílio do manejo de irrigação racional.

Palavras-Chave: agricultura digital, modelagem de pragas, modelagem de doenças, manejo de irrigação, dados em grid, *Sacharum spp.*

Modeling tools for stakeholders in Smart Agriculture

ABSTRACT - Agriculture in the world is moving at a high speed towards the next green revolution, the so-called digital agriculture revolution, which combines other major areas that have revolutionized agriculture, such as biotechnology and precision agriculture. These techniques were essential for increasing agricultural productivity in the world. Digital agriculture can now further optimize the association of climatic data in crop planning and crop management. The concept of "Smart Agriculture" is embedded in the world of digital agriculture as a promising and necessary line for the sustainable future of agriculture. This work presents management strategies for sugarcane producing areas, such as (i) a process-based model system for predicting the susceptibility of orange rust, based on weather conditions; (ii) estimation of infestation of *Mahanarva fimbriolata* by artificial neural networks; (iii) a smartphone application to estimate potential evapotranspiration using grid weather data from the NASA-POWER system. The strategies proposed in this work proved to be efficient and promising for practical application. The orange rust model accurately simulated the orange rust severity index, and provided the expansion of the simulations, with the objective of verifying the susceptibility of the disease occurrence in large areas of sugarcane production, such as Brazil, India and Australia. The use of artificial neural networks to estimate infestation levels of *Mahanarva fimbriolata* has been shown to be a viable and promising alternative. The estimation of potential evapotranspiration, using grid meteorological data from NASA-POWER, obtained results with high accuracy and precision, thus making the smartphone application developed a tool to aid rational irrigation management.

KEYWORDS: digital agriculture, pest modeling, disease modeling, irrigation management, gridded data, *Sacharum spp.*

CAPÍTULO 1 - Considerações Gerais

A agricultura é a atividade econômica que mais é influenciada pelas condições climáticas sendo que o clima afeta todas as etapas do cultivo, desde o preparo do solo para semeadura, até colheita, além dos controles fitossanitários, manejo de irrigação, transporte e armazenamento dos produtos. Qualquer alteração no clima terá um impacto sobre o crescimento e desenvolvimento da cultura, bem como na ocorrência de pragas e doenças nas plantas.

O aumento populacional e a demanda por alimentos incentivam cada vez mais os pesquisadores, profissionais da área e investidores, a compreender as relações entre o clima e a produção agrícola. Nesse âmbito surgem tecnologias e novos conceitos, como o de “Smart Agriculture”, para auxiliar no entendimento da relação entre clima e produção, visando soluções economicamente viáveis e sustentáveis.

O conceito de “Smart Agriculture” (agricultura inteligente – tradução livre) envolve a ciência de dados e uma combinação multidisciplinar de várias ferramentas para relacionar grande quantidade de dados e informações pertinentes auxiliando na gestão antecipada e automatizada das atividades agrícolas (Prototop e Shanoyan, 2016; Ribarics, 2016; Carolan, 2018).

Dentro do conceito de “Smart Agriculture”, um dos grandes desafios da comunidade científica é atender a crescente demanda por ferramentas que auxiliem os tomadores de decisão no manejo agrícola de forma mais sustentável. Este fato chama cada vez mais atenção para a necessidade de modelos de simulação confiáveis que identifiquem os riscos e estime a produtividade, assim como as perdas referentes aos estresses bióticos e os impactos causados na qualidade da produção (Bregaglio e Donatelli, 2015).

As perdas na produção agrícola devido a ocorrência de pragas e doenças pode chegar até aproximadamente 16% da produção mundial de alimentos (Oerke, 2006; Garret et al., 2013). O impacto causado por pragas e doenças é ainda incerto devido as mudanças no clima e ao elevado número de fatores ambientais e de manejo que interagem contribuindo para o aumento de epidemias (Coakley et al., 1999; Chakraborty e Newton, 2011). A quantificação destes impactos de pragas e doenças sob diferentes intensidades representa uma das questões de pesquisa mais

importantes para a modelagem de simulação agrícola (Savary et al., 2006; Whish et al., 2015).

Os modelos de simulação fornecem aos gestores de terras e formuladores de políticas uma ferramenta para extrapolar os resultados experimentais (Basso et al., 2013), auxiliam no manejo adequado das pragas e doenças, gerando alertas fitossanitários, resultando em menor custo de produção, menor contaminação do ambiente, melhoria na qualidade do produto agrícola além da diminuição no uso de defensivos agrícolas. Os modelos de simulação possibilitam ainda a previsão de disseminação potencial das doenças e pragas de plantas, aumentando ainda mais a contribuição da agrometeorologia para o controle fitossanitário racional.

O Brasil é o maior produtor mundial de cana-de-açúcar (*Saccharum* spp.) (FAO, 2018), o que faz com que a cana seja considerada um dos principais produtos do agronegócio brasileiro. Atualmente, conta com uma área plantada de mais de dez milhões de hectares. A produção nacional na última safra, 2017/2018, foi superior a 737 milhões de toneladas (IBGE, 2018). A importância consolidada da cana-de-açúcar para o mercado brasileiro exige que estratégias de manejo sejam desenvolvidas como modelos que simulem e estimem o impacto de pragas e doenças.

Devido a grande complexidade e do grande número de elementos que se interagem nos sistemas de produção, outro grande desafio dentro do conceito de “Smart Agriculture” está relacionado ao uso correto da água. A Agricultura é de longe o setor que mais demanda água, respondendo por cerca de 70% de toda a água retirada de rios e aquíferos em todo o mundo para produção agrícola (Siebert et al., 2013).

Ahmad e Prasad (2012) afirmam que 45% das áreas agrícolas do mundo sofrem com a seca. A quantidade de água em boa qualidade existente no ambiente é finita e sua disponibilidade diminui gradativamente devido ao crescimento populacional, à expansão das fronteiras agrícolas e à degradação do ambiente. Sendo a água um recurso indispensável à vida, é de fundamental importância a discussão das relações entre o homem e a água, uma vez que a sobrevivência das gerações futuras depende diretamente das decisões que hoje estão sendo tomadas. O uso da água de forma descontrolada pode comprometer os recursos hídricos (Silva et al.,

2016), além de elevar os custos da produção tornando o manejo adequado da irrigação racionalizada uma ferramenta fundamental e indispensável neste processo.

Neste contexto, as tecnologias associadas a “Smart Agriculture” são potencialmente os maiores aceleradores de tecnologias de produção agrícola desde a Revolução Verde, de acordo com o Fórum de Economia Mundial - World Economic Forum (2016). Esta fusão da ciência de dados e agricultura poderá ajudar produtores, pesquisadores e profissionais do setor a tomar decisões baseadas na otimização da produtividade, aumento da receita e minimização de custos (Rosenzweig et al., 2013; Capalbo et al., 2017; Antle et al., 2017; Rao, 2018).

Este estudo busca apresentar técnicas para abordagem “Smart Agriculture” com foco em áreas de cultivo da cana-de-açúcar. Nos próximos capítulos serão apresentadas ferramentas de suporte para auxílio na gestão de áreas agrícolas em geral (irrigação) e para o setor canavieiro (sistemas de suporte a decisão fitossanitária).

REFERÊNCIAS

Ahmad P, Prasad MNV (2012) Environmental Adaptations and Stress Tolerance of Plants in the Era of Climate Change. Springer. 515 p.

Antle JM, Jones JW, and Rosenzweig CE (2017) Next generation agricultural system data, models and knowledge products: Introduction, **Agricultural Systems**, 155: 179–185.

Basso B, Cammarano D, Carfagna E (2013) Review of crop yield forecasting methods and early warning systems. In Proceedings of the First Meeting of the Scientific Advisory Committee of the Global Strategy to Improve Agricultural and Rural Statistics, FAO Headquarters, Rome, Italy, 18–19 July 2013.

Bregaglio S, Donatelli MA (2015) A set of software components for the simulation of plant airborne diseases. **Environ. Model. Softw**. 72: 426–444.

Capalbo SM, Antle JM, Seavert C (2017) Next generation data systems and knowledge products to support agricultural producers and science-based policy decision making, **Agricultural Systems**, 155:191-99.

Carolan M (2018) **The Politics of Big Data: Corporate Agri-Food Governance Meets “Weak” Resistance.** In Agrienvironmental Governance as an Assemblage:

Multiplicity, Power, and Transformation, edited by Jeremie Forney, Chris Rosin, and Hugh Campbell, London: Routledge, 195–212.

Chakraborty S, Newton AC (2011) Climate change, plant diseases and food security: an overview. **Plant Pathol.** 60: 2-14.

Coakley SM, Scherm H, Chakraborty S (1999) Climate change and plant disease management. **Annu. Rev. Phytopathol**. 37: 399-426.

FOOD AND AGRICULTURE ORGANIZATION OF THE UNITED NATIONS - FAO (2018). Production. Disponível em: http://faostat3.fao.org/home/E Acesso em: 20 de ago. 2018.

Garrett KA, Dobson ADM, Kroschel J, Natarajan B, Orlandini S, Tonnang HEZ, Valdivia C (2013) The effects of climate variability and the color of weather time series on agricultural diseases and pests, and on decisions for their management. **Agric. For. Meteorol.** 170: 216-227.

INSTITUTO BRASILEIRO DE GEOGRAFIA E ESTATÍSTICA – IBGE (2015) Estatísticas sobre Agricultura. Disponível em http://www.sidra.ibge.gov.br/bda/agric/default.asp?z=t&o=11&i=P Acesso em: 19 ago. 2018.

Oerke EC (2006) Crop losses to pests**. J. Agric. Sci.** 144: 31-43.

Protopop I, Shanoyan A (2016) Big Data and Smallholder Farmers: Big Data Applications in the Agri-Food Supply Chain in Developing Countries. **International Food and Agribusiness Management Review** 19 (A): 173–90.

Rao NH (2018) Big Data and Climate Smart Agriculture - Status and Implications for Agricultural Research and Innovation in India, **Proceedings of the Indian National Science Academy**, 1-32.

Ribarics P (2016) Big Data and Its Impact on Agriculture. **Ecocycles** 2 (1):33–34.

Rosenzweig C, Jones JW, Hatfield JL, Ruan AC, Boote KJ, Thorburn P, Antle JM, Nelson GC, Porter C, Janssen S, Asseng S, Basso B, Ewert F, Wallach D, Baigorria G, Winter JM (2013) The Agricultural Model Intercomparison and Improvement Project (AgMIP): Protocols and pilot studies, **Agricultural and Forest Meteorology**, 170: 166–182.

Savary S, Teng PS, Willocquet L, Nutter JRFW (2006) Quantification and modeling of crop losses: a review of purposes. **Annu. Rev. Phytopathol**. 44: 89–112.

Siebert S, Henrich V, Frenken K, Burke J (2013) **Update of the Global Map of Irrigation Areas to version 5.** Project report, 178 p.

Silva ECR, Alves FB, Silva IIS (2016) Irrigated agriculture in the Amazon context: A systematic approach to the use of water in a horticulture in the municipality of Atamira-PA. **Revista Internacional de Ciências** 6(1): 29–43.

Whish JPM, Herrmann NI, White NA, Moore AD, Kriticos DJ (2015) Integrating pest population models with biophysical crop models to better represent the farm ing system. **Environ Model. Softw.** 72: 418–425.

World Economic Forum (2016). The Global Risks Report, 11th Edition, World Economic Forum, Geneva, Switzerland, 103 pp.

CAPÍTULO 2 - A model-based system to predict the favorability of weather conditions for orange rust disease of sugarcane

ABSTRACT- The improvement and application of disease models to analyze the impacts on crops is still a challenge for the scientific community. Process-based models appears to represent a viable methodology to estimate the impacts of these potential effects, since a new generation of tools based on state-of-art knowledge is needed to allow systems analysis including key processes and their dynamics over appropriate suitable range of environmental variables. We identified the key processes in the epidemiological cycle of the *Puccinia kuehii* and developed a new process-based model to simulate the orange rust intensity index (ARISE). With the objective to analyze the suitability we applied the process-based model developed in large areas in Brazil, India and Australia for twenty years. The results showed that the model performed robustly, it simulated the classification of severity indices accurately and confirmed that the weather requirements for the development of orange rust are high temperatures and relative humidity. The percentage of hit of the model in simulating the presence or absence of the disease was 90%, while to classify the presence of disease in high or low severity was 61%. With careful calibration and validation to other sites, climates and fungal disease, it may become a valuable tool in the assessment of disease impacts in food security and appropriate control measures, providing an integrated management.

KEYWORDS: *Puccinia kuehnii*, disease modeling, process-based model, severity index

Sistema de estimativa da favorabilidade à ferrugem alaranjada em cana-de-açúcar baseado em modelos mecanísticos em função das condições meteorológicas

RESUMO- A melhoria e aplicação de modelos para analisar os impactos de doenças nas culturas ainda é um desafio para a comunidade científica. Os modelos mecanísticos representam uma metodologia viável para estimar esses impactos, uma vez que uma nova geração de ferramentas baseadas no atual estado da arte do conhecimento permiti a análise de sistemas, incluindo processos chave e a dinâmica do patógeno com um conjunto apropriado de variáveis ambientais. Foram Identificados os principais processos no ciclo epidemiológico do fungo *Puccinia kuenhii*, agente causal da ferrugem alaranjada, e foi desenvolvido um novo modelo baseado nos processos para simular o índice de severidade da ferrugem alaranjada (ARISE). Com o objetivo de analisar a predisposição da doença, o modelo desenvolvido foi aplicado em grandes áreas no Brasil, na Índia e na Austrália durante vinte anos. Os resultados mostraram que o modelo foi robusto, simulou a classificação

dos níveis de severidade com precisão e confirmou que os principais fatores predisponentes para a ocorrência da doença são, alta temperatura e umidade relativa. A porcentagem de acertos do modelo em simular a presença ou ausência da doença foi de 90%, enquanto que para classificar a presença de doença em alta ou baixa severidade foi de 61%. Com cuidadosa calibração e validação para outros locais, climas e doenças fúngicas, este trabalho pode se tornar uma ferramenta valiosa na avaliação dos impactos de doenças na segurança alimentar e em medidas de controle apropriadas, proporcionando um manejo integrado.

PALAVRAS-CHAVE: *Puccinia kuehnii*, modelagem de doença, índice de severidade.

INTRODUCTION

Plant diseases are responsible for major economic losses in the agricultural industry worldwide. The orange rust caused by the polycyclic fungal pathogen *Puccinia kuehnii* (W. Krüger) E. J. Butler (1914) is a relatively new emerging biotic constraint to sugarcane cultivation worldwide (Magarey, 2000; Sentelhas et al., 2016). Firstly reported by Krüger in 1890 on sugarcane fields in the Java Island, orange rust disease arrived in the Western Hemisphere as a result of global trade (Rott et al., 2016). In 2009 the pathogen was detected in São Paulo state, Brazil (Barbasso et al., 2010) from where it spread across the main sugarcane harvested areas in the northeast regions (Chaves et al., 2013). Nowadays, orange rust is considered the most emerging threat to sugarcane health in Brazil, which is the top sugarcane producing and exporting country (Bordonal et al., 2018), with an annual production of 615 million tons (CONAB, 2019).

According to Araújo et al. (2013), yield losses due to orange rust in susceptible and moderately resistant varieties can be higher than 40%, and sugarcane growers try to limit these impacts by planting resistant varieties. However, several resistance breakdowns have been observed and alternative control methods, such as chemical control, are needed. Three to four fungicide applications are required per growing season to keep orange rust under an economical threshold (Rott et al., 2016). Additional strategies to counteract the impacts of the disease are currently being investigated, including the shift of the planting date, since the environmental conditions is the main driver of orange rust (Chaulagain et al., 2019), while a disease warning system to support in-season management is not yet available.

Puccinia kuehnii is a Basidiomycete, from the Uredinales order and Pucciniaceae family (Hauksworth et al., 1995). Symptoms of orange rust include yellow flecks, reddish brown elongated lesions, and oval shaped orange-brown pustules releasing urediniospores (Rott et al., 2016) leading to reduced net photosynthetic rates, stomatal conductance, and transpiration (Zhao et al., 2011). The epidemiology of orange rust of sugarcane largely depends on environmental conditions, with high moisture and warm temperatures favoring the increase of disease severity (Magarey, 2000; Minchio et al., 2017). The life cycle begins with the infection process, which consists in the germination of a urediniospore producing a germ tube able to penetrate the sugarcane leaves through stomata (Nalwar, 2013). Optimum temperatures for infection range between 22 and 24 °C, with elevated relative humidity prolonging leaf wetness duration (Magarey et al., 2004). The leaves are asymptomatic up to the end of the latency process, when a pustule on the underside of the leaf, cinnamon to orange color, become visible and starts to sporulate (Magarey, 2000). The latency period ranges from 10 to 21 days and its duration strictly depends on air temperature (Moreira et al., 2018). After this stage, pustules progressively open and produce the urediniospores which are released into the air and are dispersed by wind. The optimal conditions for the sporulation process are temperature between 19 to 26 °C and very high relative humidity (above 98%), with wind speed playing a major role for spore dispersal from one region to another (Ferrari et al., 2013).

The orange rust occurrence in Brazil is relatively recent but the evolutionary potential is already known due to capability to rapidly mutate and overcome host resistance of the current sugarcane varieties. Recent laboratory studies indeed support the existence of pathogenic variants of the orange rust pathogen in Florida (Sanjel et al., 2016). The development of a reliable early warning system based on process-based simulation model would then support both in-season management with timely indications on the risk of infection and could also provide medium-term forecasts of the pathogen pressure in order to plan investments for new sugar mills. Simulation models have indeed the potential to provide tools to extrapolate experimental results from one site to another (Basso et al., 2013), thus enabling the generation of alerts based on weather conditions, making possible the prediction of the potential impact and diffusion of the simulated diseases (Gillespie and Sentelhas, 2008).

In this paper we present a model-based index of sugarcane orange rust favorability (ARISE, orAnge Rust IntenSity indEx) which reproduces the key process of the epidemiological cycle of *Puccinia kuhenii*, i.e., *onset* of the disease, *infection*, *spore dispersal*, *latency* and *sporulation*. ARISE was calibrated and validated using 857 observations of disease severity collected in 3-year field surveys in Brazil, and then applied on the main Brazilian, Indian and Australian sugarcane production area in order to provide in-season and long-term scenario analyses of disease intensity.

MATERIAL AND METHODS

Process-based models in ARISE

The ARISE index provides a dynamic simulation of the main processes underlying the epidemiological cycle of *Puccinia kuehnii* and integrates them to give a synthetic measure of sugarcane orange rust severity. ARISE consists in a chain of simulation models reproducing the timing of the symptom's onset, and the processes of infection, spore dispersal, latency duration and sporulation efficiency (Figure 1).

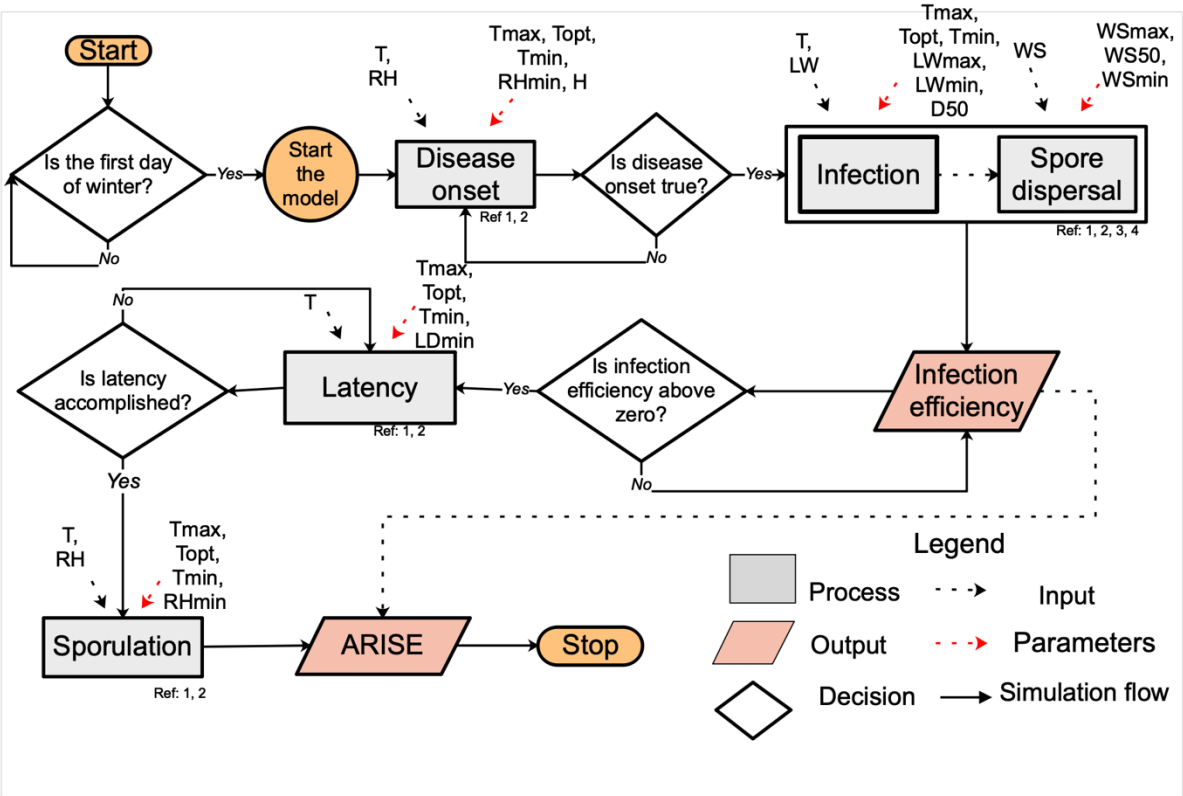

[1] Bregaglio and Donatelli (2015); [2] Yan and Hunt (1999); [3] Magarey et al. (2005); [4] Aylor (1982).

Figure 1. Conceptual diagram of the processes simulated by the ARISE model-based index. T (ºC), temperature; Tmax (ºC), maximum temperature; Topt (ºC) optimal temperature; Tmin (ºC), minimum temperature; RH (%), relative humidity; RHmin (%), minimum relative humidity; H (hour), threshold; LW (true/false), leaf wetness; LWmax (hour), maximum leaf wetness; LWmin (hour), minimum leaf wetness; D50 (hour), dry period; WS (m s^{-1}), wind speed; WSmax (m s^{-1}), maximum wind speed; WSmin (m s^{-1}), minimum wind speed; WS50 (m s^{-1}), wind speed for dispersion of 50% of spores; LDmin (hour), latency duration minimum; ARISE (unitless), orAnge, Rust IntenSity indEx.

Most of the process-based models implemented in ARISE have got a hourly time step: the model workflow starts in the first day of winter, when a hourly rate of primary inoculum is computed as a function of thermal and moisture requirements. Once the accumulated rate of disease onset reaches a given threshold, the suitability of weather conditions for the infection process starts to be simulated, together with the

efficiency of spore dispersal as driven by daily wind speed. ARISE considers that each infection event passes through the latency period, whose duration varies according to air temperature. When the latency period is accomplished, the efficiency of the sporulation process is simulated as a function of relative humidity and thermal conditions, and it is integrated to give the ARISE index. All the models implemented in ARISE are presented in Table 1, with their inputs, outputs and parameters.

Table 1. Acronym, description, unit and literature source of the values of the parameters needed to reproduce the epidemiological cycle of *Puccinia kuehnii* in the ARISE model-based index.

Parameters	Description	Unit	Reference[a]
TmaxDO	Maximum temperature for disease onset	°C	1, 2, 3, 4, 5, 6, 8
ToptDO	Optimum temperature for disease onset	°C	1, 2, 3, 4, 5, 6, 7, 8
TminDO	Minimum temperature for disease onset	°C	1, 2, 3, 4, 5, 6, 8
RHminDO	Relative humidity minimum for disease onset	%	1, 7
H	Threshold necessary for disease onset	unitless	
TmaxInf	Maximum temperature for infection	°C	1, 2, 3, 4, 5, 6, 8
ToptInf	Optimum temperature for infection	°C	1, 2, 3, 4, 5, 6, 7, 8
TminInf	Minimum temperature for infection	°C	1, 2, 3, 4, 5, 6, 8
LWmax	Not limiting leaf wetness duration for infection	h	
LWmin	Minimum leaf wetness for infection	h	5, 6, 8
D50	Dry hours to stop an infection event	h	
WSmax	Maximum wind speed for dispersal	m s^{-1}	9, 10
WS50	Wind speed for dispersal 50% of spores	m s^{-1}	
WSmin	Minimum wind speed for dispersal	m s^{-1}	9, 10
TmaxL	Maximum temperature for latency	°C	1, 2, 3, 4, 5, 6, 8

			1, 2, 3, 4, 5, 6, 7,
ToptL	Optimum temperature for latency	°C	8
TminL	Minimum temperature for latency	°C	1, 2, 3, 4, 5, 6, 8
LDmin	Latency duration minimum	day	8, 11
TmaxS	Maximum temperature for sporulation	°C	12
ToptS	Optimum temperature for sporulation	°C	12
TminS	Minimum temperature for sporulation	°C	12
RHminS	Minimum relative humidity for sporulation	%	

[a]1: Infante et al. (2009); 2: Hsieh et al. (1977); 3: Minchio et al. (2011); 4: Minchio et al. (2017); 5: Vasudeva (1958); 6: Lima et al. (2017); 7: Magarey et al. (2004); 8: Martins (2010); 9: Ferrari et al. (2013); 10: Mallaiah and Rao (1982); 11: Moreira et al (2017); 12: Hsieh et al. (1983).

The main purpose of the model of *disease onset* is to determine the initial day of appearance of orange rust symptoms. This model is based on the accumulation of hydro-thermal time (Bregaglio and Donatelli, 2015), with the day of disease onset set when the state variable related to disease onset (DOstate, d, unitless, Eq. 1) reaches a threshold of hydro-thermal time requirement (H, unitless, Eq. 1). DOstate, Equation (2), is in turn computed as the accumulation of the hourly rate variable DO rate (h, unitless), which starts to be computed on the first day of winter. DOrate is simulated as a function of hourly air temperature and hourly air relative humidity (Eq. 3). The temperature response function (f(T), unitless, 0 -1) is reported in Equation (4) (Yan and Hunt, 1999).

$$DOstate,\ d > H \tag{1}$$

$$DOstate,\ d = \sum_{n-1}^{24} DOrat \tag{2}$$

$$DOrate,\ h = \begin{cases} 0\ \ if\ \ \ RH < RHt \\ f(T)\ \ elsewhere \end{cases} \tag{3}$$

$$f(T) = \left(\frac{Tmax - T}{Tmax - Topt}\right)\left(\frac{T - Tmin}{Topt - Tmin}\right)^{\left(\frac{Topt - Tmin}{Tmax - Topt}\right)} \tag{4}$$

where RH (%) is hourly air relative humidity, RHt (%) is the threshold of air relative humidity which inhibits inoculum development (Schoeny et al., 2007), T (°C) is hourly air temperature, Tmin, Tmax and Topt (°C) are pathogen specific cardinal temperatures for the development of primary inoculum.

The simulation of the *infection process* is based on the suitability of thermal and moisture conditions in the form of leaf wetness duration for *Puccinia kuehnii*. The generic model for airborne fungal pathogens developed by Magarey et al. (2005) was parameterized according to literature data and used in ARISE. This model computes the air temperature response function (f(T), Equation (4)) and scales it to the pathogen specific wetness duration requirement, according to Equation (5).

$$\mathrm{f}(LW) = \begin{cases} \frac{LWmin}{f(T)} & if \quad \frac{LWmin}{f(T)} \leq LWmax \\ 0 & elsewhere \end{cases} \tag{5}$$

where f(LW) (h) is the leaf wetness response function, LWmin (h) is the minimum leaf wetness duration for infection, and LWmax (h) is the leaf wetness duration not limiting the completion of an infection event. The model considers the impact of a dry period on the infection process by means of a critical interruption value (D50, h), as reported in Equation (6) (Bregaglio and Donatelli 2015):

$$Wsum = \begin{cases} W_1 + W_2 & D < D50 \\ W_1, W_2 & elsewhere \end{cases} \tag{6}$$

where Wsum (h) is the cumulated duration of a leaf wetness period and W1 and W2 (h) are two wet periods separated by an interruption (D, h). The model considers two wet periods as separated if D ≥ D50. An infection event is fulfilled when the duration of Wsum is above f(T); if Wsum < f(W), the infection event remains incomplete and it is evaluated at the next hour.

The third model in ARISE computes the efficiency of *spore dispersal*, which is simulated on a daily time step according to Aylor (1982), as a function of average wind speed (Equations 7-10):

$$\mathrm{f}(SD) = \begin{cases} 0 & if \quad WS < WSmin \\ \frac{(WS - WSmin)^2}{(WS - WSmin)^2 + (Ws50 - WSmin)^2} & if \quad WSmin \leq WS \leq WS50 \\ \frac{(WS - WSmin)^2}{(WS - WSmin)^2 + (WS50 - WSmin)^2 \, c} & if \quad WS50 < WS \leq WSmax \\ 1 & if \quad WS > WSmax \end{cases} \tag{7}$$

$$c = b + a\,WS \tag{8}$$

$$b = 1 - a\,WS50 \tag{9}$$

$$a = \frac{1}{WSmax - WS50} \tag{10}$$

where WS (m s^{-1}) is daily wind speed, WSmin (m s^{-1}) is the minimum wind speed for spore dispersal, WS50 (m s^{-1}) is the wind speed for the dispersal of 50% of spores, WSmax (m s^{-1}) is the wind speed for the maximum spore dispersal. The term c (unitless) is used to assign the maximum wind dispersal when WS is equal to WSmax, b (unitless) and a (m s^{-1}).

The efficiency of the infection process is then calculated by multiplying the number of infection events in a day by the spore dispersal efficiency (Equation 11). The duration of latency period is then computed starting from each hour when infection efficiency is above zero. The duration of the latency period is determined basing on air temperature, considering the minimum number of hours required at optimum temperature.

$$Infection\ Efficiency = Number\ of\ infection\ events * Spore\ Dispersal \tag{11}$$

$$Latency\ Completion = (LDmin) + (LDmin * (1 - f(T)) \tag{12}$$

where LDmin (hour) is the minimum duration of the latency period. When the latency period is accomplished, the host tissue starts to become infectious and sporulates producing the secondary inoculum. The last model implemented in ARISE indeed simulates the efficiency of sporulation considering hourly relative humidity and temperature as driving variables (Equation 13).

$$Sporulation\ Efficiency = \begin{cases} f(T) & if \quad RH \geq RHmin \\ 0 & elsewhere \end{cases} \quad (13)$$

where RH (%) is hourly relative humidity and RHmin is minimum relative humidity for sporulation. The ARISE index is computed as the final step of the modelling chain (daily, unitless) according to Equation (14). The description and sources of information of the parameters used to describe the epidemiological cycle of *Puccinia kuehnii* are listed in Table 1.

$$ARISE, d = \sum_{i=0}^{24}(InfectionEfficiency * SporulationEfficiency) \quad (14)$$

Sources of data for model calibration and validation

The ARISE index was calibrated and validated using reference data of orange rust severity collected during field surveys. The disease severity rust was assessed on seventy farms in Pradópolis region, state of São Paulo in 2016-2018, for a total of 857 observations. The data were provided by private companies in the region (Figure 2). Two independent operators conducted the field surveys by sampling five plants in each plot and giving an overall score od disease severity after sampling five plants in different plots of the field. The orange rust severity was estimated by considering the lower middle third of leaf +3 according to the diagnostic scale established by the Copersucar Center for Phytopathology Coordination (Amorim et al., 1987). This scale corresponds to the resistance level of the species based on the percentage of leaf limbus destroyed by rust, varying from 1 to 9 (Amorim et al., 1987). The field samplings were performed in plots where sugarcane varieties were considered susceptible to orange rust.

Daily meteorological data needed as input for ARISE were downloaded from the NASA-POWER database (NASA, 2018), they were daily values of maximum and minimum air temperature (°C); maximum and minimum air relative humidity (%); average wind speed (m s^{-1}) and dew temperature (°C). The NASA-POWER project was developed to provide meteorological information for direct use for architecture, power generation and agrometeorology in a horizontal resolution of 0.5 × 0.5°. The

meteorological data are based upon a single assimilation model from Goddard's Global Modeling and Assimilation Office (GMAO).

With the aim to test the capability of ARISE to be applied across other sugarcane growing areas, we made a spatial analyze in three large areas producers of sugarcane, Brazil, India and Australia. These areas were chosen since they are important producers of sugarcane, have already reported problems with orange rust and because of the different climatic conditions. We downloaded 20 years (1997 – 2017) of weather data from NASA-POWER, for these three regions. The number of grid cells corresponding to the main sugarcane producer in Brazil were 1,819, whereas in India and Australia were downloaded 505 and 419 grid cells, respectively. The spatial analyze was made with the mean value of ARISE, mean air temperature and relative humidity in the 20 years. Yearly and ten-day period temporal resolution were also analyzed, through a animation chart, with the purpose of analyzing the evolution of ARISE over the years and during an epistemological cycle.

Given the need to adopt a hourly time step for most of the simulated processes by ARISE index, we had to generate hourly values starting from daily data. Hourly air temperature was then estimated from daily maximum and minimum air temperature using the models developed by Campbell (1985), whereas hourly air relative humidity was derived according to Bregaglio et al. (2010), based on models proposed by Linacre (1992), Allen et al. (1998) and ASAE (1998). Hourly wind speed was estimated according to Donatelli et al. (2009), based on model proposed by Tartako et al. (1997). Hourly leaf wetness was estimated from hourly air temperature, dew point temperature, wind speed and relative humidity, by using the approach proposed by Kim et al. (2002). All these models make use of sub-models implemented in the software components AirTemperature (Donatelli et al., 2010), EvapoTranspiration (Donatelli et al., 2006), Wind (Donatelli et al., 2009), all included in CLIMA weather generator (Donatelli et al., 2009).

Simulation experiment design

The ARISE index was calibrated and validated using reference data of sugarcane orange rust severity collected during the field surveys, before projecting it

on large areas to assess weather suitability on main sugarcane producing countries. A literature search was performed to retrieve the values of the epidemiological parameters measured in laboratory or field experiments, and the corresponding ranges were used to perform automatic model calibration of their values to maximize model accuracy. The automatic optimization was performed using the multi-start simplex algorithm as implemented by Acutis and Confalonieri (2006), the simplex is a geometrical concept, consisting of N + 1 vertices in a N-dimensional space. The simplex moves through a multidimensional space according to reflection, contraction, and expansion, according to the gradient of the objective function, until a minimum (usually the absolute one) is reached.

The values of ARISE were translated into a disease score in order to compare it with field samplings of disease severity. The reference data of orange rust severity ranged between 1 (disease severity = 0%) to 6 (disease severity = 25%, Table 2).

The simulated and observed data of orange rust severity were compared (i) using all disease scores from 1 to 6, (ii) dividing them into absence (disease score = 1) and presence of disease (disease score from 2 to 6) and (iii) dividing them into low (disease score 2 and 3) and high (disease score from 4 to 6) orange rust severity.

Table 2. Disease score and subjective classification of orange rust according to diagnostic scale established by the Copersucar Center for Phytopathology Coordination (Amorim et al., 1987; Cda, 2010).

Disease Score	Classification	% disease severity
1	Absence of disease	< 0.5
2	Low disease	0.5
3		1
4	High disease	5
5		10
6		< 25

Model performances in reproducing observed disease scores were quantified through contingency tables. In this tables, a *hit* indicates that both reference observation and simulation detected the event, whereas a *miss* occurs when the event is identified by reference observation, but it is missed by the simulation. *False alarm*

then represents an event which is simulated but not confirmed by observation and a *correct negative* represents an event which is not detected in simulations and observations (AghaKouchak and Mehran 2013). The following metrics were then computed based on the on the contingency tables: the probability of detection (POD) (Eq. 15) which describes the fraction of the reference observations correctly identified by the simulation; the false alarm ratio (FAR) (Eq. 16) which corresponds to the fraction of events identified by simulation but not confirmed by reference observations; critical success index (CSI) (Eq. 17), which combines different aspects of the POD and FAR, describing the overall skill of the simulation relative to reference observation; and accuracy (Eq. 18), which is the ratio of the correctly classified observations by the total number of cases.

$$POD = \frac{hit}{hit+miss} \quad (15)$$

$$FAR = \frac{false}{hit+false} \quad (16)$$

$$CSI = \frac{hit}{hit+miss+false} \quad (17)$$

$$Accuracy = \frac{hit+correct\ negative}{total} \quad (18)$$

RESULTS

Accuracy of ARISE in reproducing field data

The ARISE index obtained similar and positive performances in calibration and validation datasets both in the evaluation of presence-absence of orange rust disease and in the classification of low and high disease severity and the cardinal temperatures and moisture requirements for the different phases of the epidemiologic cycle were varied according to literature data (Table 3). The percentage of complete matches between simulated and observed data in calibration dataset considering presence-absence of orange rust disease was 90% (296 data), in which 80% were classified as

hits, i.e., correct reproduction of presence of the disease and 10% as correct negatives, i.e., correct reproduction of absence of the disease. The percentage of false alarm was 9%, meaning that ARISE overestimated the presence of orange rust. The percentage of misses was negligible (1%) (Fig. 2). The Accuracy and POD in the evaluation of orange rust presence-absence were 0.91, whereas the FAR and the CSI were 0.01 and 0.90 (Table 4).

The ability of ARISE in reproducing high and low orange rust disease severity was lower. According to this evaluation criterion, the percentage of complete matches in calibration was 61% (264 data), with 27% of hits and 34% correct negatives. The percentages of false alarms and misses were 18% and 21%, respectively. The ability of ARISE in reproducing high and low orange rust disease severity was lower with 0.65 of accuracy, POD = 0.46, FAR = 0.41 and CSI = 0.35. ARISE performances in validation agreed with the ones obtained in calibration datasets, with a higher complete percentage of matches in reproducing presence-absence of disease than in identifying high and low orange rust disease severity (Figure 2). Considering the ability of ARISE in reproducing the different scales of orange rust severity, the percentage of complete matches between simulated and observed data was 33.20% (98 observations) on the whole datasets (296), whereas the percentage of errors of ±1 and ±2 on the rust severity scale was 39.6% and 20% (117 and 61 data). Larger errors were significantly less frequent, with only 5% and 0.5% of data with errors of ±3 and ±4 on the scale (Figure 3).

Table 3. Optimized parameters values, units and the ranges (Minimum, Maximum) used to calibrate the epidemiology of *Puccinia kuehnii*. The description of the acronyms of the parameters is reported in Table 1.

Parameters	Unit	Minimum	Maximum	Optimazed
TmaxDO	°C	25.0	34.0	29.9
ToptDO	°C	18.0	25.9	22.4
TminDO	°C	8.0	17.0	10.5
RHminDO	%	70.0	90.0	80.6
H	unitless	16.00	20.00	18.5
TmaxInf	°C	25.0	34.0	29.9
ToptInf	°C	18.0	25.9	22.4
TminInf	°C	8.0	17.0	10.5

LWmax	h	18.0	20.0	18.8
LWmin	h	7.0	9.0	7.8
LW50	h	2.0	4.0	3.1
WSmax	m s^{-1}	4.0	4.4	4.2
WS50	m s^{-1}	2.4	2.7	2.5
WSmin	m s^{-1}	0.6	0.9	0.7
TmaxL	°C	25.0	34.0	29.9
ToptL	°C	18.0	25.9	22.4
TminL	°C	8.0	17.0	10.5
LDmin	day	14.0	17.0	15.3
TmaxS	°C	29.5	30.5	29.9
ToptS	°C	26.9	27.9	27.6
TminS	°C	22.2	23.2	22.6
RHminS	%	78.0	84.0	80.6

Table 4. Summary statistics of the comparison between simulated and observed data of orange rust disease severity in calibration and validation dataset. Legend: POD, probability of detection; FAR, false alarm ratio; CSI, critical success index.

	Calibration				Validation			
	POD	FAR	CSI	Accuracy	POD	FAR	CSI	Accuracy
Presence and absence of disease	0.90	0.01	0.89	0.90	0.93	0.02	0.92	0.93
High and low disease	0.55	0.41	0.40	0.61	0.38	0.42	0.30	0.65

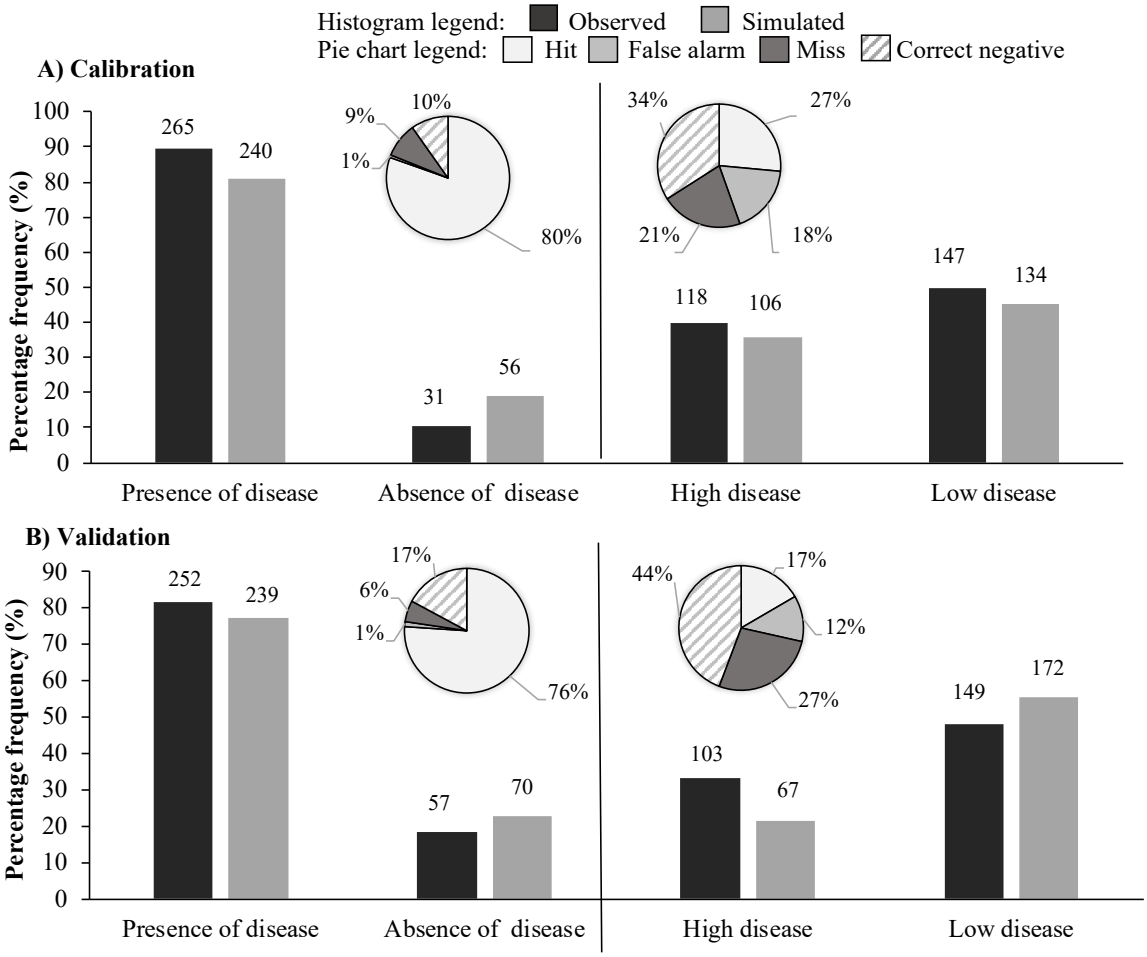

Figure 2. Results of the comparison between simulated and observed data considering the two evaluation criteria of presence-absence of orange rust (left figures) and low-high rust disease severity (right figures) in calibration (A) and Validation (B) datasets. The Histograms refer to the percentage frequency of observed (black) and simulated (gray) disease score, whereas pie charts report the percentages of hits, false alarms, misses and correct negatives obtained in the two evaluation criteria.

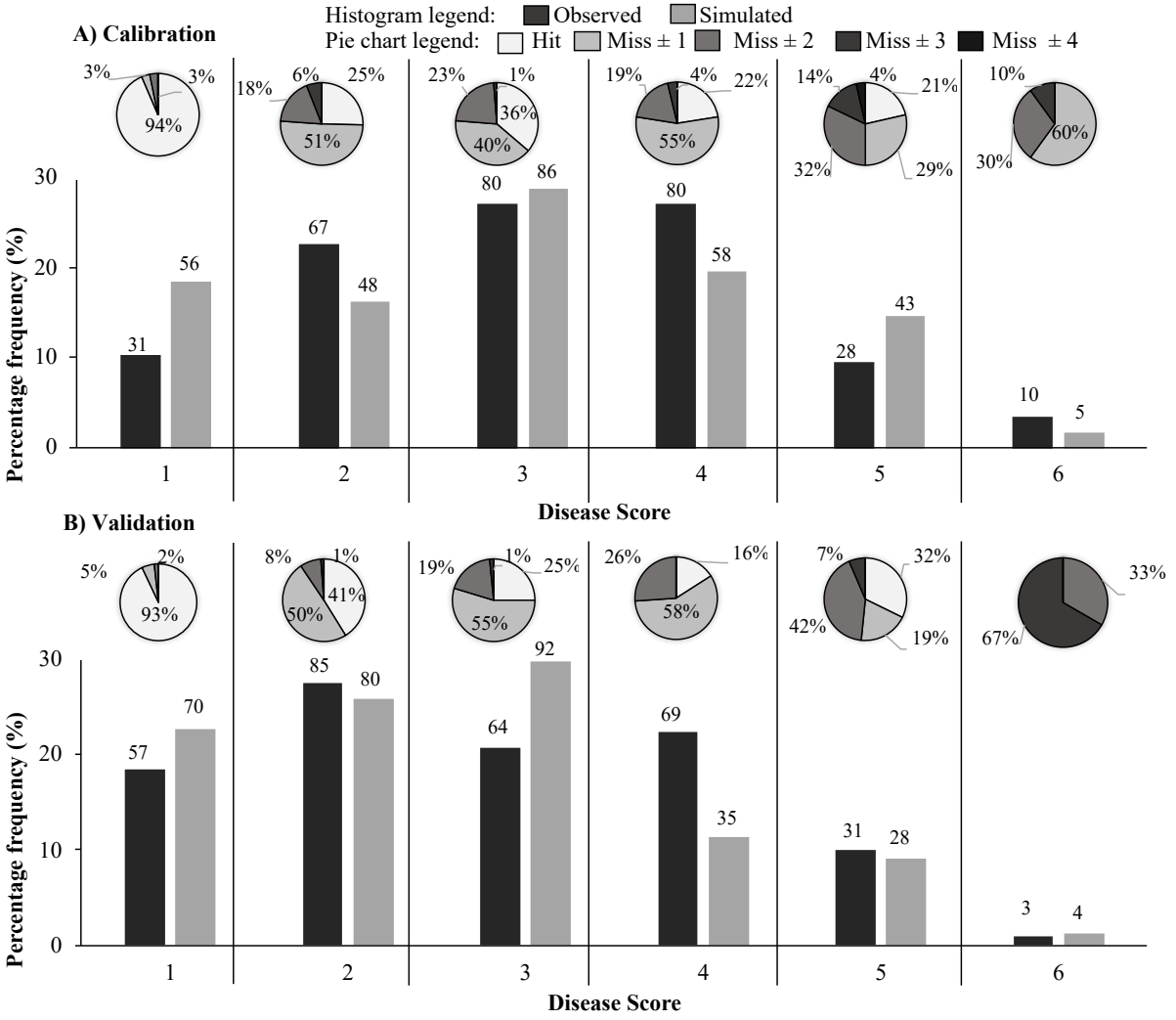

Figure 3. Results of the comparison of simulated values of disease score with observed ones on the A) Calibration and B) Validation dataset. Histograms refer to the percentage frequency of observed (black) and simulated (gray) disease score, whereas pie charts depict the type of error made by the modelling solution for each score of the orange rust assessment scale.

Analyzing ARISE response during the growing season

The distributions of ARISE values (lines, median and standard errors) in the three years where observations were carried out, obtained using input data from the weather grids of the NASA-POWER database corresponding to the sugarcane fields where field surveys were carried out (points and bars, average values and standard errors) showed that the behavior of the model solution matches with the measured

data. Although there was a delay in the model in detecting the presence of disease in 2016, the model had no problems in detecting when low disease became high disease, which in the three years occurred in February (Figure 4).

The distribution of the data observed was a limitation in this study, since the number of observed data, in the period of 2016/2017, was higher. However, beside this limitation, the model response was assertive and presents a low variability associated. In the cycle of 2017/2018, the number of observations was the lowest, while the severity of orange rust was the highest, and the model was able to capture this information. This result confirms that the calibrated parameters are robust since they were able to reproduce the severity index of the orange rust in function of the variability of the humidity and temperature conditions.

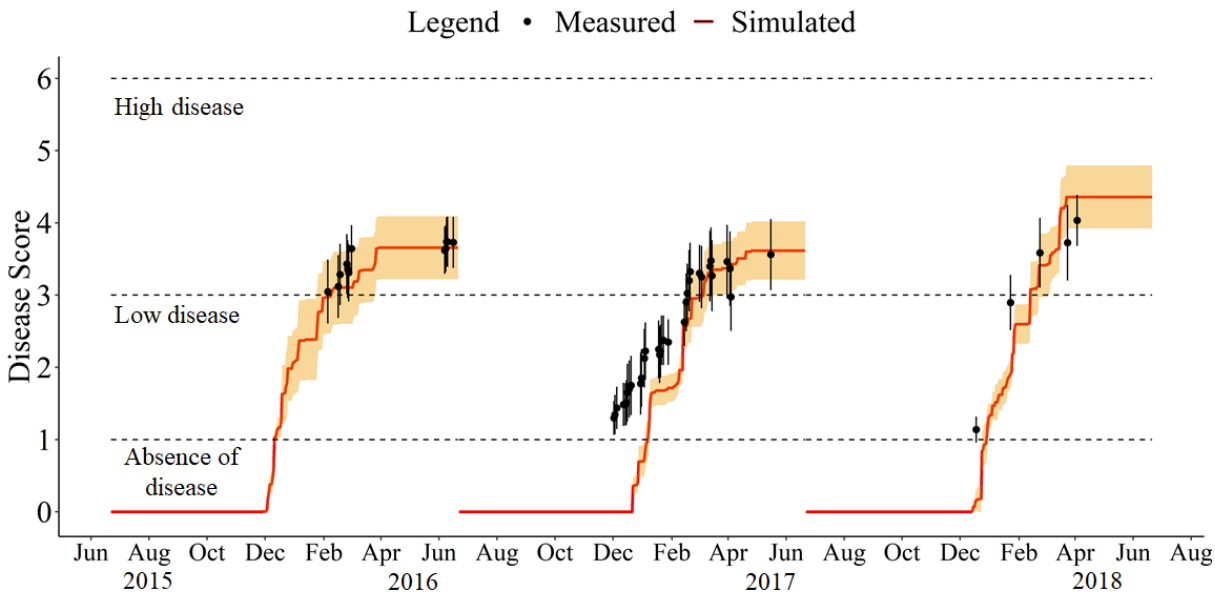

Figure 4. Results of the comparison between simulated (solid lines) and observed disease data (circles) referred to orange rust for the three epidemiologic cycle of *Puccinia kuehnii*. The variability of the simulated (orange ribbon) and measured (error bar) data are represented by the standard error.

The outputs obtained in the simulated processes present the distribution curves of the inputs used thermal and moisture conditions and the outputs generated in the simulation according to the epidemiological cycle of the *Puccinia kuehnii*, from 1997 to 2017, responded to a pattern according to the temperature and moisture conditions

(Figure 5). The onset disease rate started with low values in the months of July, August and September, where temperature and leaf wetness were also low. In October, when there was an increase in temperature and number of leaf wetness hours, occurred an increase in the disease onset rate and as a consequence in the number of infection events. The latency process in the months with lower temperatures and leaf wetness hours was higher, reaching up to 25 days, while in the months of high temperatures and leaf wetness hours it was approximately 20 days. The combination of the thermal and moisture conditions and the simulation responses resulted in lower values of ARISE up to November, with a gradual increase in the distribution in December, and higher values from January to the end of the epidemiological cycle, in June.

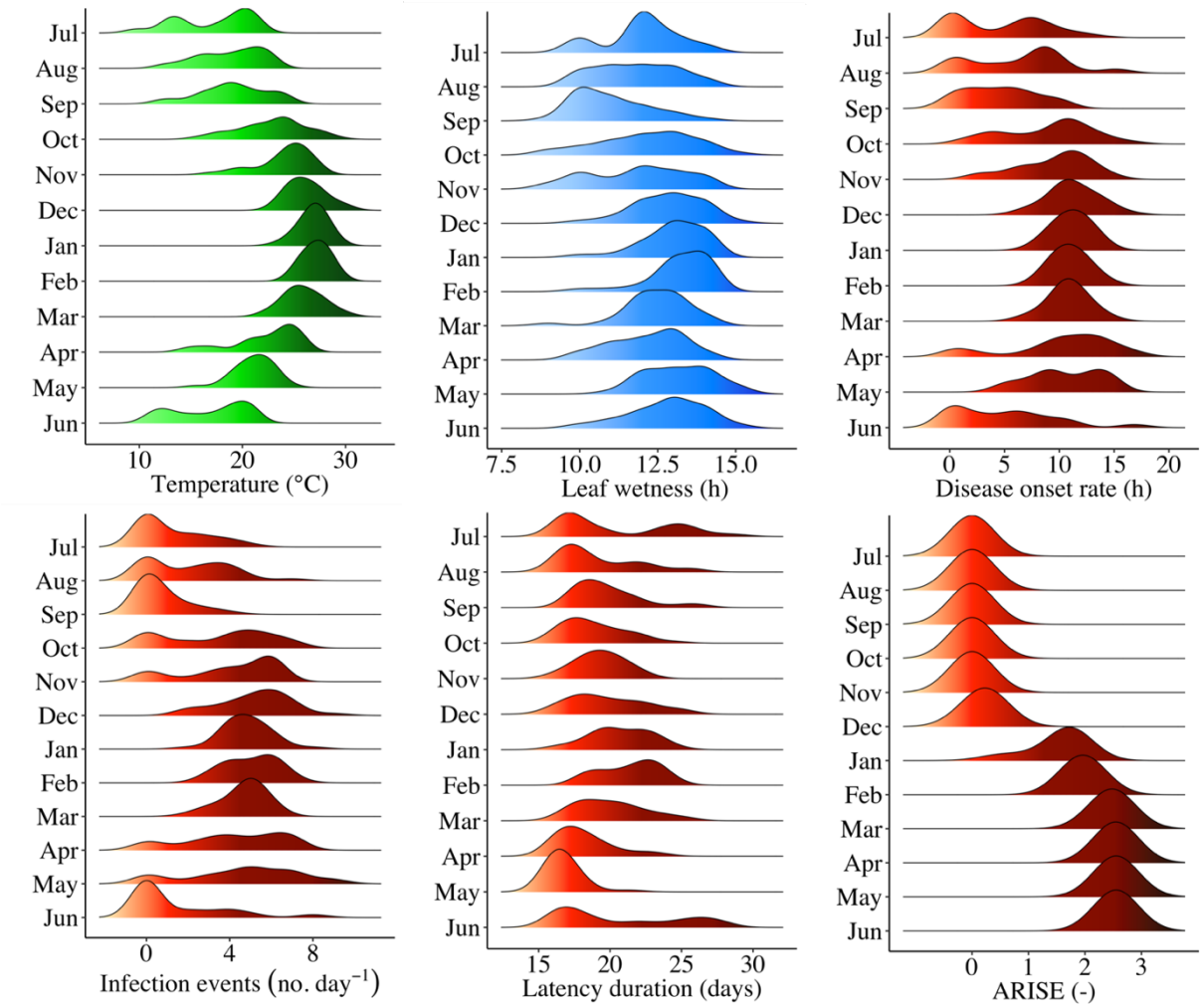

Figure 5. Distribution curve for average values in 20 years of hourly temperature, hourly leaf wetness, disease onset rate, number of infection events, latency duration

and ARISE, results from the model response, in the following coordinates 25° 15’ 0” S, 54° 15’ 0” W.

Spatial applications of ARISE across sugarcane growing areas

The spatialization of the simulated values (ARISE), average relative humidity and air temperature, for Brazil, India and Australia taking in account the 20 years studied (Figure 6), shows that India was potentially more favorable to orange rust and that this fact is linked to the highest values of average air temperature. The optimal temperature for the development of orange rust calibrated was 22 °C with maximum value of 29 °C, in India the mean value of temperature was between this range in almost all the cells grids studied.

Since in Brazil, some regions, e.g. the South, the mean temperature was near to 14 °C and the ARISE responded to this condition with low values even with high relative humidity in this region. Therefore, we can infer that the average temperature has more influence in the simulation of ARISE in India and Brazil. On the other hand, Australia, followed relative humidity, since the highest values were found in the coastal areas.

The spatial analyze in the ten-day period and annual (20 years) scale can be found in the supplementary material in the form of animation. Analyzing the temporal distribution of the 10-day scale, the first values of ARISE occurs only in November in Brazilian northeastern region, an important producer of sugarcane. Only in December that the phenomenon begins in the center-west region and in the region of São Paulo, Brazil's main sugar cane production. In India, the first ARISE values begin in the first month of simulation, July, as in Brazil, begins in the coastal region and then distributes to the others, always with high values. In Australia, the response was similar to the others, starting in September in the coastal areas. In the annual scale animation (1997-2017), we found that ARISE in most of the years was simulated in the same regions, there were some alternations between higher and lower indexes, but it occurred in the same places and in India the values were always high, confirming the high favorability of India to Orange rust.

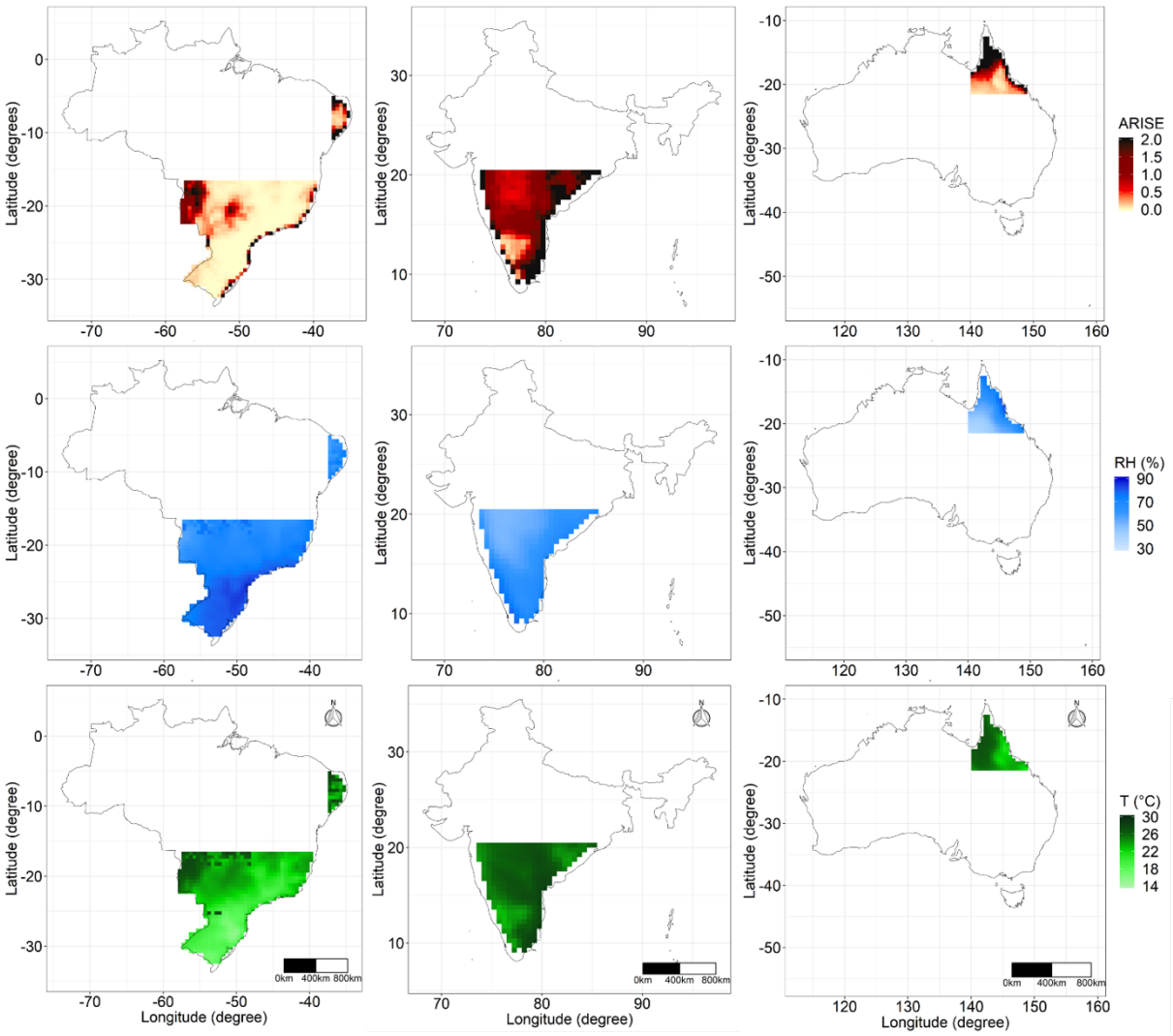

Figure 6. Spatialization of the mean simulated values (ARISE), relative humidity (RH, %) and temperature (T, °C) for large areas in Brazil, India and Australia from 1997 to 2017.

DISCUSSION

Diseases are limiting factors for the sugarcane crop in almost any sugarcane growing location (Root et al., 2016) and the impact of the severity caused by disease are uncertain due to climate changes and the high number of environmental and management factors driving the occurrence of disease (Chakraborty and Newton, 2011). Orange rust is a real concern, since the main control is done by resistant

cultivars obtained through breeding and several resistance breakdowns have been observed (Root et al., 2016). These breakdowns were attributed to development of new races of the pathogen, suggesting constant evolution and adaptation of *P. kuehnii* (Chaulagain et al., 2019). Therefore, alternative control methods, such as application of fungicides, associated with a decision tool for help the stakeholders in forecasting disease progress and optimize the application of fungicides are needed Root et al. (2016). No decision support model for sugarcane orange rust based on environmental conditions was found in the literature.

We developed a model-based index called ARISE which simulates the predisposition of weather conditions for sugarcane orange rust disease, which combines process-based models of the components of the epidemiologic cycle of *Puccinia kuehnii*. We focused on the key process of the epidemiologic cycle for developing ARISE, the timing of the symptom's onset, infection, spore dispersal, latency duration and sporulation efficiency. Specific information about the life cycle of *Puccinia kuehnii* has not been found in the literature, however in this work we rely on information about another fungus of the same gender, which also causes serious problems in sugarcane, *Puccinia melanocephala*. According to Nalwar (2013), the life cycle starts with the germination of a urediniospore to produce a germ tube. Formation of an appresorium follows after the germ tube comes into contact with a stoma them a short penetration peg, which enters through the stomatal aperture, was formed. Following, occur the infection hyphae development and starts colonized the leaf and grow intercellularly until the epidermis subsequently ruptured by a mass of urediniospores (Purdy et al., 1983). We adapted generic process-based models with parameterization taken from literature data for simulate these key components of the *Puccinia kuehnii* epidemiologic cycle.

The cardinal temperatures and moisture requirements for the different phases of the epidemiologic cycle calibrated were varied according to literature data. The optimum, maximum and minimum temperature for the initial development of inoculum, infection and latency obtained in the present work were 22, 30 and 10 °C. This result agrees with those obtained in laboratory experiments performed by Infante et al. (2009); Magarey et al. (2004); Martins et al. (2010) and Michio et al. (2017), which

verified that the range of temperature for the development of this fungus is between 10 and 30 °C, with optimal near to 22 °C. For sporulation, a higher sensitivity was observed with minimum and optimum temperature of 22 and 27 °C, as it was found by Hsieh and Fang (1981), minimum and maximum of 22 and 30 °C, respectively. The moisture requirements were 80% of relative humidity and 7 hours of leaf wetness. These results are very close those founded by Infante et al. (2009) and Magarey et al. (2004), with 97 and 98 % of relative humidity and 8 hours of leaf wetness as observed by Martins et al. (2010). The values of wind speed, maximum, minimum for spore dispersal were 4 and 0.7 m s^{-1}. The latency period at optimum temperature were set to 15 days, one day less them that found by Martins et al. (2010).

The results obtained in this work showed that the model obtained good performances in the simulation of the severity index of orange rust, in the region of São Paulo. Comparing the simulated and observed data, we observed that ARISE detected with accuracy and precision the presence and absence of the disease and for the differentiation of the disease in low or high, the performance was satisfactory. For decision makers, it is extremely important to know exactly the best time to perform disease control, so the ability of the model to simulate the presence of disease is presented as a reliable alternative. According to Chaulagain et al. (2019), in a experiment realized in Florida, testing the application timing of fungicides for the management of sugarcane orange rust, fungicide applications at the beginning of epidemics resulted in the lowest rust progress values during the sugarcane crop season. Since the applications at mid or late epidemic stage were less, but they were still useful for partial control of orange rust.

The process-based model was able to reproduce the main process of the fungus, according to the thermal and moisture requirements and obtained satisfactory results in simulate the severity index. These results confirm that environment conditions that favor the occurrence of the disease are high air relative humidity and high temperatures (Magarey, 2000; Minchio et al., 2017).

In the suitability analyze, the model was able to reproduce the severity index in larger areas, as in this study, where we simulated the Severity Index (ARISE) for large areas in Brazil, India and Australia, all sugarcane producers. Yield losses were

reported in Australia as high as 50%, and direct monetary losses were estimated at 200 million Australian dollars for the period 2000–2001 (Magarey et al., 2011). Since the evolutionary potential is not known, the suitability in large areas and in longer periods is very important for understanding the behavior of the fungus in different geographical and climate conditions. Recent laboratory investigations support the existence of pathogenic variants of the orange rust pathogen in Florida (Sanjel et al., 2016).

Despite the overall very satisfactory performance of the model, some main criticalities have to be faced. The main one is the resolution of weather data used as input, which has a grid cell of 0.5 ° x 0.5 °, corresponding approximately 50 km^2, the best scenario would be localized weather stations near the points sampled. However, due to the size of the territorial extension, Brazil does not have a network that meets all the needs (Pereira et al., 2002). The parameters used in calibration are other criticalities, were either taken or deduced from literature all describing laboratory, i.e. ideal condition, which can differ greatly from the reality of the producers. However, should new data ever become available, the model can easily be adapted to include the new information. To minimize this risk of including weather effects in the values of the parameters of the disease model and could improve model performances is the availability of high-quality input data, especially hourly temperature and leaf wetness.

Another issue is the uncertainty related to the assessment of the observed data, which deterred us from further calibrating the model to achieve a closer fit. The low number of observations with high scores also caused a bias in the model, where the accuracy in the simulation of high and low disease was lower. However, in situations where there is greater variability of the data, with higher severity indexes, this model can be easily calibrated. Scale is another criticality since the model response, ARISE, are continues values and the observed value is a point scale, due to this fact was necessary translate the ARISE in to disease score, for comparing the simulated with observed data.

Besides these criticalities, it should be noted that this model currently applies to only one specific fungal disease, however, it can be applied and calibrated to other

fungal diseases that cause damages in other crops, aiming at an integrated management of diseases.

CONCLUSIONS

The use of process-based models to simulate the key processes of the epidemiology of *Puccinia kuehnii* can be a viable tool in the integrated management of this disease, since it accurately simulated the severity index of orange rust in sugarcane. The spatialization analysis confirms that the calibration of the parameters was robust and corroborates that orange rust is a disease mainly driven by thermal and moisture conditions. Going forward, the features and abilities of this process-based model as whole ecosystem model make it a potential tool for running climate scenarios on future, to study the impact of the climate change in the pressure of diseases.

REFERENCES

Acutis M, Confalonieri R (2006) Optimization algorithms for calibrating cropping systems simulation models. A case study with simplex-derived methods integrated in the WARM simulation environment. **Italian Journal of Agrometeorology**, 3: 26 – 34.

AghaKouchak A, Mehran A (2013) Extended contingency table: Performance metrics for satellite observations and climate model simulations. **Water Resources Research**, 49: 7144-7149.

Allen RG, Pereira LS, Raes D, Smith M (1998) Crop evapotranspiration: guidelines for computing crop water requirements. **Irrig Drain** 56, 300 pp. UN-FAO, Rome, Italy

Amorim L, Bergamin Filho A, Sanguino A, Ardoso COM, Moraes VA, Fernandes CR (1987) Metodologia de avaliação de ferrugem da cana-de-açúcar (*Puccinia melanocephala*). Boletim Técnico Copersucar: São Paulo, 39: 13-16.

Araújo KL, Canteri MG, Gilio TAS, Neubauer RA, Sanches PB, Sumida CH, Giglioti EA (2013) Genotypic resistance and monitoring of favorability for the occurrence of orange rust in sugarcane. **Summa Phytopathologica**, 39(4): 271-275.

ASAE Standards (1998) EP406.2: heating, cooling, and ventilating greenhouses. St. Joseph, MI, USA

Aylor DE (1982) Modelling spore dispersal in a barley crop. **Agric. Meteorol.** 26: 215-219.

Barbasso D, Jordão H, Maccheroni W, Boldini J, Bressiani J, Sanguino A (2010) First report of Puccinia kuenhii, causal agent of orange rust of sugarcane, in Brazil. **Plant Disease** 94:1170.

Basso B, Cammarano D, Carfagna E (2013) Review of crop yield forecasting methods and early warning systems. In Proceedings of the First Meeting of the Scientific Advisory Committee of the Global Strategy to Improve Agricultural and Rural Statistics, FAO Headquarters, Rome, Italy 18-19

Bordonal RO, Carvalho JLN, Lal R, Figueiredo EB, Oliveira BG, La Scala Jr N (2018) Sustainalility of sugarcane production in Brazil. A review. **Agron. Sustain. Dev.** 38: 13. https://doi.org/10.1007/s13593-018-0490-x

Bregaglio S, Donatelli M (2015) A set of software components for the simulation of plant airbone diseases. **Environmental Modelling & Software**, 1-9. http://dx.doi.org/10.1016/j.envsoft.2015.05.011.

Bregaglio S, Donatelli M, Confalonieri R, Acutis M, Orlandini S (2010) An integrated evaluation of thirteen modelling solutions for the generation of hourly values of air relative humidity**. Theor Appl Climatol**, 102: 429.

Chakraborty S, Newton AC (2011) Climate change, plant diseases and food security: an overview. **Plant Pathol.** 60: 2-14.

Campbell GS (1985) **Soil Physics With BASIC: Transport Models for Soil–Plant Systems**. Elsevier, Amsterdam, The Netherlands.

Chaulagain B, Raid RN, Dufault N, Van Santen E, Rott P (2019) Application timing of fungicides for the management of sugarcane orange rust, **Crop Protection**, 119: 141-146.

Chaves A, Simões Neto DE, Dutra Filho JA, Oliveira AC, Rodrigues WDL, Pedrosa EMR, Borges VJL, França PRP (2013) Presence of Orange rust on sugarcane in the state of Pernambuco, Brazil. **Tropical Plant Pathology**, 38(5): 443-446.

CONAB - Companhia Nacional de Abastecimento (2019), Observatório Agrícola: Acompanhamento da safra brasileira (Cana-de-açúcar) Terceiro levantamento (Safra 2018/2019), 5(3). Disponível em: https://www.conab.gov.br/info-agro/safras/cana/boletim-da-safra-de-cana-de-acucar Acesso em: 07/04/2019.

Donatelli M, Bellocchi G, Carlini L (2006) Sharing knowledge via software components: models on reference evapotranspiration. **Eur J Agron** 24:186–192

Donatelli M, Bellocchi G, Habyarimana E, Bregaglio S, Baruth B (2010) AirTemperature: extensible software library to generate air temperature data. **SRX Computer Science** (in press)

Donatelli M, Bellocchi G, Habyarimana E, Bregaglio S, Confalonieri R, Baruth B (2009) CLIMA, a modular weather generator. In: Anderssen RS, Braddock RD, Newham LTH (eds) 18th World IMACS Congress and MODSIM09 International Congress on Modelling and Simulation. Modelling and Simulation Society of Australia and New Zealand and International Association for Mathematics and Computers in Simulation. July 2009, pp 852– 858. ISBN: 978-0-9758400-7-8. http://www.mssanz.org.au/ modsim09/C3/donatelli_C3a.pdf

Donatelli M, Bellocchi G, Habyarimana E, Confalonieri R, Micale F (2009) An extensible model library for generating wind speed data. **Computers and Electronics in Agriculture**, 69(2): 165-170.

Ferrari JT, Harakava R, Domingues RJ, Terçariol IML, Töfoli JG (2013) Orange rust of sugarcane in Brazil. **Biológico**, São Paulo, 75(1): 71-74.

Gillespie TJ, Sentelhas PC (2008). Agrometeorology and plant disease management – a happy marriage. **Scientia Agricola**, 65: 71-75.

Hawksworth DL, Kirk PM, Sutton BC, Pegler DN (1995) Ainsworth & Bisby's dictionary of the fungi. 8. ed. Wallingford:CAB international.

Hsieh WH, Fang JB (1981) Studies on sugarcane rust disease. 1980-81 **Annu Rep. Taiwan Sugar Res.** Inst., pp. 22-23.

Hsieh WH, Fang JG (1983) The uredospore production of *Puccinia melanocephala* and *Puccinia kuehnii* in sugarcanes. **Plant Prot. Bull.**, 25(4): 239-244.

Hsieh WH, Lee CS, Chan SI (1977) Rust disease of sugarcane in Taiwan: the causal organism *Puccinia melanocephala* Sydow. **Taiwan Sugar**, 24(5): 416-410.

Infante D, Martinez B, Gonzalez E, Gonzalez N (2009) *Puccinia kuehnii* (Kruger) Butler y *Puccinia melanocephala* H. Sydow y P. Sydow en el cultivo de la caña de azúcar. **Revista Protección Vegetal**, 24:22-28.

Kim KS, Taylor SE, Gleason ML, Koehler KJ (2002) Model to enhance site-specific estimation of leaf wetness duration. **Plant Dis** 86:179–185

Lima LL, Scaloppi EAG, Barreto LF, Barreto M (2017) Temperatures and leaf wetness duration on orange rust development in sugarcane (*Puccinia kuehnii*). **Summa Phytopathologica**, 43(2): 132-135.

Linacre E (1992) **Climate data and resources: a reference and guide.** Routledge, London

Magarey RC (2000). **Orange rust**. In: Rott, P., Bailey, R.A., Comstock, J.C., Croft, B.J., Girad, J- C. and Saumtally, S. (eds). A Guide to Sugarcane Diseases, 121–125. CIRAD – ISSCT: Montpellier, France.

Magarey RC, Neilsen WA, Magnanini AJ (2004) Environmental requirements for spore germination in the three sugarcane leaf pathogens. In: Conference of the Australasian Society of Sugar Cane Technologists held at Brisbane, Queensland, 1-7.

Magarey RD, Sutton TB, Thayer CL (2005) A simple generic infection model for foliar fungal plant pathogens. **Phytopathology**, 95: 92-100.

Mallaiah KS, Rao AS (1982) Aerial dissemination of groundnut rust uredinospores. **Transactions of the British Mycological Society**, 82: 21-28.

Martins TD (2010) Aspecto epidemiológico da ferrugem alaranjada da cana-de-açúcar. 2010, 65f. **Tese** (Doutorado em Fitopatologia) – Escola Superior de Agricultura " Luiz de Queiroz", Universidade de São Paulo, Piracicaba, 2010.

Minchio CA, Canteri MG, Rocha JA (2011) Germinação de uredósporos de Puccinia kuehnii submetidos a diferentes temperaturas e tempos de incubação. **Summa Phytopathologica**, 37(4): 211-214.

Minchio CA, Fantin LH, Oliveira KB, Rocha JA, Canteri M (2017) Morphological changes of the Urediniospore of Puccinia kuehnii germ tube in function of temperature. **Agronomy Science and Biotechnology**, 3:19-24.

Moreira AS, Nogueira Junior AF, Gonçalves CRNB, Souza NA, Bergamin Filho A (2018) Pathogenic and molecular copmparison of Puccinia kuehnii isolates and reacyions of sugarcane varieties to Orange rust. **Plant Pathology**, 67(8): 1687-1696.

Nalwar SE (2013) Epidemiology and management of sugarcane rust caused by *Puccinia melanocephala* H. and P. Syd. (**Master dissertation**), University of Agricultural Sciences, august, 2013.

NASA (2018) NASA surface meteorology and solar energy: Methodology. NASA. https://power.larc.nasa.gov/documents/POWER_Data_v9_methodology (accessed 8 April. 2018).

Pereira AR, Angelocci LR, Sentelhas PC (2002) **Agrometeorology: Fundamentals and practical applications**. Agropecuária, Guaíba.

Purdy LH, Liu L, Dean JL (1983) Sugarcane rust, a newly important disease. **Plant Dis.**, 69: 1292-1296.

Rott PC, Kaye C, Naranjo, M, M Shine Jr J, Sood S, Comstock JC, Raid RN (2016) Controlling sugarcane diseases in Florida: a challenge in constant evolution**. Proc. Int. Soc. Sugar Cane Technol**. 29: 595-600.

Sanjel S, Hincapie M, Sood S, Comstock JC, Raid RN, Rott P (2016) Evidence for variation in virulence of the sugarcane orange rust pathogen in Florida. 46th American Society of Sugar Cane Technologists Annual Meeting, 13–15 June 2016, St Pete Beach, FL. Sugar Journal 79(1): 29–30.

Schoeny A, Jumel S, Rouault F, Le May C, Tivoli B (2007) Assessment of airborne primary inoculum availability and modelling of disease onset of ascochyta blight in field peas. **Eur. J. Plant Pathol.** 119: 87-97.

Sentelhas PC, Santos DL, Monteiro LA, Soares-Colletti AR, Pallone Filho WJ, Donzelli JL, Arrigoni EB (2016) Agro-climatic favorability zones for sugarcane orange rust as a tool for cultivar choice and disease management. **Crop protection**, 84, 88-97.

Tatarko J, Skidmore EL, Wagner LE (1997) Wind erosion prediction system: weather generator submodel. In: Wind Erosion: An International Symposium/Workshop Commemorating the 50th Anniversary of USDA-ARS Wind Erosion Research, Manhattan, KS, USA, http://www.weru.ksu.edu/ symposium/proceedings/tatarko.pdf.

Vaseduva RS (1958) Report of the division of mycology and pathology. Sci. Rep. agric. Res. Inst. N. Delhi. 1956-1957. **Rev. Appl. Mycol.** 86-100.

Yan W, Hunt LA (1999) An equation for modelling the temperature response of plants using only the cardinal temperatures. **Ann. Bot.** 84: 607-614.

Zhao D, Glynn NC, Glaz B, Comstock JC, Sood S (2011) Orange rust effects on leaf photosynthesis and related characters of sugarcane. **Plant Dis.** 95, 640-647.

CAPÍTULO 3- Estimativa da Infestação de *Mahanarva fimbriolata* na cultura da cana-de-açúcar por meio de Redes Neurais Artificiais

RESUMO- A classificação dos níveis de infestação de pragas é de extrema importância, pois auxilia os tomadores de decisão na gestão correta e de forma mais sustentável. O Brasil é o maior produtor de cana-de-açúcar e uma das maiores causas de perdas na produtividade é a ocorrência de pragas como a cigarrinha-das-raízes (*Mahanarva fimbriolata*). Para tanto tem se tornado cada vez mais necessário a busca de novas tecnologias. As redes neurais artificiais (RNAs) são uma ferramenta que vem se destacando no desenvolvimento dos modelos preditivos para estimar parâmetros necessários. O objetivo deste estudo foi de gerar RNAs capazes de estimar a classificação dos índices de infestação de *Mahanarva fimbriolata* em cana-de-açúcar, em função de variáveis climáticas. Os dados de infestação da praga foram fornecidos por empresas da mesorregião de Jaboticabal – SP. Os dados climáticos utilizados foram provenientes do projeto NASA-POWER, que disponibiliza estes dados em Grid em escala diária e uma resolução de 0,5º x 0,5°. A estratégia utilizada na construção das redes neurais para classificar a pressão populacional de cigarrinha foi a Automatic Network Search (ANS). Foram geradas um total de quatro tipos de RNAs duas Radial Basis Fuction, uma Multilayer Perception e uma rede neural linear, sendo que a Radial Basis Fuction com 21 neurônios foi a que obteve um melhor desempenho para previsão do nível de infestação.

Palavras-chave: RNA, Multilayer Perception, Radial Basis Fuction, cigarrinha-das-raízes.

Estimation of *Mahanarva fimbriolata* infestation in sugarcane culture through artificial neural networks

ABSTRACT: Classification of pest infestation levels is extremely important, as it assists decision-makers in the correct management and in a more sustainable way. Brazil is the largest producer of sugarcane and one of the major causes of losses in yield is the occurrence of pests such as the rootworm (*Mahanarva fimbriolata*). For that, it has become increasingly necessary to search for new technologies. Artificial neural networks (ANNs) are a tool that has been emphasizing the development of predictive models to estimate necessary parameters. The main of this study was to generate RNAs capable of estimating the classification of infestation rates of *Mahanarva fimbriolata* in sugarcane, as a function of climatic variables. The pest infestation data were provided by companies from the Jaboticabal - SP mesoregion. The climatic data used came from the NASA-POWER project, which provides this data in Grid on a daily scale and a resolution of 0.5 x 0.5°. The strategy used in the

construction of neural networks to classify the population pressure of spittlebugs was Automatic Network Search (ANS). A total of four types of RNAs were generated: Radial Basis Fuction, Multilayer Perception and a linear neural network, and Radial Basis Fuction with 21 neurons was the one with the superior performance.

Keywords: RNA, Multilayer Perception, Radial Basis Fuction, spittlebug.

INTRODUÇÃO

O Brasil é o maior produtor mundial de cana-de-açúcar (*Saccharum spp*.) (FAO, 2016), o que faz com a mesma seja considerada um dos principais produtos do agronegócio brasileiro. Dentre as principais pragas desta cultura, destaca-se a Cigarrinha, *Mahanarva sp.* (Hemiptera: Cercopidae), (Dinardo-Miranda, 2014). Responsável por perdas de até 44,8% na produtividade agrícola e na qualidade da matéria-prima, com reduções de até 30% no teor de sacarose (Dinardo-Miranda et al., 2001)

O impacto dessas severidades é incerto devido as mudanças no clima e ao elevado número de fatores ambientais e de gestão que interagem contribuindo para o aumento de epidemias (Coakley et al., 1999; Chakraborty e Newton, 2011). Este fato chama cada vez mais atenção para a necessidade de modelos de simulação confiáveis, para estimar o impacto de pragas e doenças em plantas (Bregaglio e Donatelli, 2015).

A quantificação dos impactos de pragas e doenças de plantas sobre o desempenho das culturas representa uma das questões de pesquisa mais importantes para a modelagem de simulação agrícola (Newman et al., 2003, Savary et al., 2006, Whish et al., 2015), pois permite gerar alertas sobre a necessidade de pulverizações com base nas condições meteorológicas, o que normalmente reduz o número de aplicações, resultando em menor custo de produção e menor contaminação do ambiente (Gillespie e Sentelhas, 2008). Entretanto de acordo com Donatelli et al. (2017) a aplicação de modelos para analisar as perdas de produtividade

devido as pragas e doenças em função das alterações climáticas, ainda é um desafio a comunidade científica.

As entradas comuns para os modelos de previsões de doenças e pragas são temperatura do ar, precipitação, umidade relativa, e duração do período de molhamento do dossel (Magarey et al., 2004), estes dados, em sua maioria, são provenientes de estações meteorológicas de superfície. Entretanto o Brasil não apresenta uma rede de estações meteorológicas que atenda todas as suas necessidades (Pereira et al., 2002). Neste contexto, os dados em grid (GD) tem ganhado destaque como fonte dos dados meteorológicos para os modelos de previsões. Exemplos de conjuntos de GD que podem ser usados para a previsão de doenças e pragas de plantas incluem o Centro de Previsão de Tempo e Estudos Climáticos (INPE/CPTEC), Centro Europeu de Previsões Meteorológicas a Médio Prazo (ECMWF) e Administração Nacional da Aeronáutica e Espaço (NASA).

Devido à complexidade do sistema agrícola, em especial a relação não linear da população de pragas com as condições climáticas, é necessário o uso de técnicas de modelagem mais avançadas (Vennila et al., 2017). Nesse contexo, as Redes Neurais Artificiais (RNA), são uma alternativa viável na busca das soluções deste desafio. Uma rede neural possui a capacidade de um cérebro humano em termos de neurônios biológicos para resolver problemas complexos ou um padrão não-linear entre conjuntos de dados de entrada e saída (Azevedo et al., 2017). Uma das vantagens desta técnica é de ser não-paramétrica, tolerar a perda de dados, e não necessitar informações detalhadas sobre o sistema a ser modelado (Silva et al., 2014).

As abordagens de rede foram aplicadas com sucesso na área agronômica como sistemas de suporte à decisão no manejo de pragas, Laxmi e Kumar (2011), desenvolveram um sistema de previsão para oídio em plantas de mostarda; Yang et al. (2007), geraram um sistema de alerta fitossanitário para míldio no pepino; Chakraborty et al. (2004), desenvolveram um modelo para a previsão da severidade de antracnose; Gaudart et al. (2004), comparou dois tipos de redes, multilayer perceptron e regressão linear para estimas dados epidemiológicos. A rede neural Multilayer perceptron (MLP) é comumente usada para modelar a dinâmica da população de pragas (Vennila et al., 2017). Entretanto, é importante enfatizar que não

foram encontrados na literatura estudos de estimações de níveis de infestação *Mahanarva fimbriolata* no cultivo de cana-de-açúcar. Diante do exposto, este estudo teve como objetivo estimar a infestação de *Mahanarva fimbriolata* no cultivo de cana-de-açúcar, em função do clima, por meio de redes neurais artificiais.

MATERIAL E MÉTODOS

Área de estudo

O local estudado foi um total de 50 fazendas na mesorregião de Jaboticabal-SP, durante os anos 2013 a 2017. Os dados de infestação de *Mahanarva fimbriolata* foram fornecidos por empresas sucroalcooleiras da região. O monitoramento da cigarrinha das raízes foi feito com base na amostragem de 6 pontos por hectare, sendo que em cada ponto a amostragem é feita em um metro de comprimento. Em cada ponto limpou-se a base da cana afastando a palha entre os colmos e dispondo-as na entrelinha para que as formas biológicas (ninfas e adultos) da praga fossem contadas e registradas. O tempo de retorno para avaliação da área foi de até 30 dias, pois a população de cigarrinha pode aumentar rapidamente em condições climáticas adequadas, e ultrapassar o nível de controle. Foi realizada a classificação dos índices de infestações em condições de baixa, média e alta pressão populacional, de acordo com a frequência da distribuição dos dados observados, considerando os quartis (Tabela 1).

Tabela 1. Estratificação das formas biológicas amostradas em classes de pressão populacional, de acordo com a distribuição da frequência dos dados amostrados.

Classes de pressão populacional	Formas biológicas (ninfas e adultos)
Baixa	< 3515 (formas biológicas ha^{-1})
Média	≤ 10068 (formas biológicas ha^{-1})
Alta	> 10068 (formas biológicas ha^{-1})

Dados meteorológicos

Os dados meteorológicos utilizados foram obtidos na plataforma NASA-POWER, que consiste em um projeto desenvolvido, para fornecer informações meteorológicas de uso direto na arquitetura, geração de energia e agrometeorologia. Este sistema compila informações de várias fontes de dados, diretamente e derivadas de GDs e disponibiliza estes dados em escala diária e com resolução espacial é de 0,5 × 0,5° (Figura 1), que corresponde a uma área de aproximadamente 55,56 × 55,56 km (Stackhouse et al., 2002).

Os elementos meteorológicos utilizados para a estimação da classificação do índice de infestação de praga por meio de Redes Neurais foram, precipitação (P, mm), temperaturas do ar absolutas máxima (TMAX, °C), mínima (TMIN, °C) e média (TMED, °C), velocidade do vento (U, m s^{-1}), umidade relativa (UR, %), temperatura no ponto de orvalho (To, °C), Radiação no topo da atmosfera (Q_0, MJ m^2 dia^{-1}) e Radiação Global Diária (Qg, MJ m^2 dia^{-1}). Foram utilizadas séries históricas de 2013 a 2017 para este estudo, estratificadas numa escala semanal.

Redes neurais artificiais (RNAs)

Uma rede neural artificial (RNA) é um modelo matemático computacional biologicamente inspirado, pois tem como base o funcionamento de um neurônio natural (Binoti et al., 2014). As RNAs são constituídas de sistemas paralelos distribuídos, compostos por unidades de processamentos simples, chamadas neurônios que processam determinadas funções matemáticas. Estes neurônios são dispostos em camadas e interligadas por um grande número de conexões, sendo estas conexões, geralmente, associadas a coeficientes denominados de pesos (Figura 1). O ajuste destes pesos é realizado por um processo chamado treinamento ou aprendizado, sendo responsável pela extração das características dos dados e armazenamento de conhecimento das redes (Binoti et al., 2014). Todos os dados foram usados no treinamento, a função de ativação foi a tangente sigmoide, com a taxa de aprendizagem variável, utilizando o erro quadrado médio como função objeto.

Para o desenvolvimento das redes, foi utilizado o Neural Networks Toolbox do software Statistica (versão 7). A estratégia utilizada na construção das redes neurais

para classificar a pressão populacional de cigarrinha foi a Automatic Network Search (ANS).

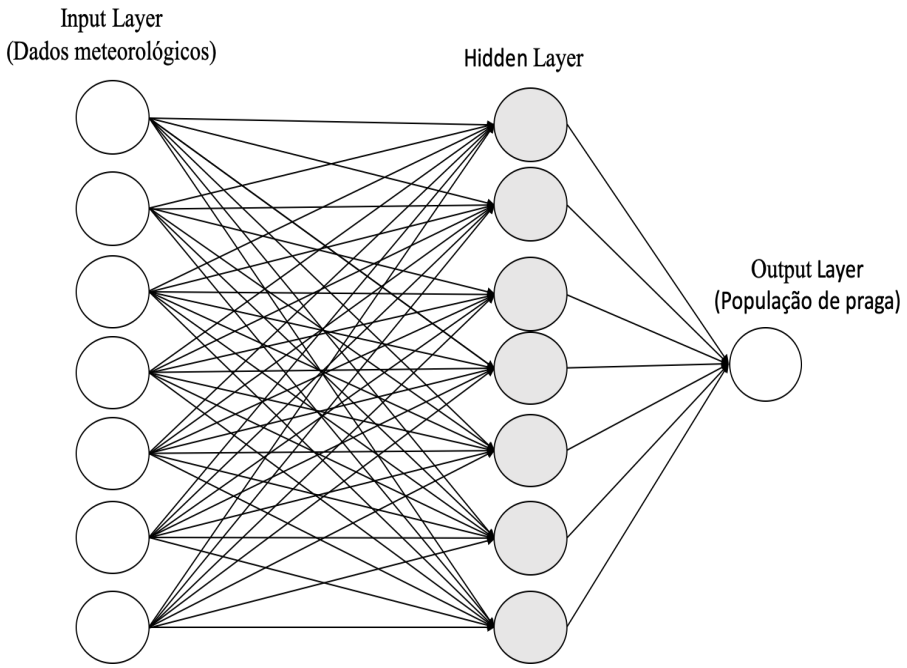

Figura 1. Exemplo da estrutura de uma rede neural artificial com uma camada de neurônios.

Análises estatísticas

A análise do desempenho das redes foi feita em duas etapas, a primeira foi realizada considerando os dados sem a estratificação em classes de pressão populacional, ou seja, avaliando o desempenho da rede em estimar o número de formas biológicas por hectare e a segunda, avaliando o desempenho das redes neurais em estimar as classes de pressão populacional. Foi realizada a estatística descritiva para os valores estimados das quatro redes neurais artificiais estudadas e o desempenho das mesmas foi avaliado de acordo com a tabela de contingência, observando o número de acertos e de erros, na classificação da infestação de cigarrinha da cana-de-açúcar em alto, médio e baixo. Uma análise de componentes principais foi feita para a rede neural artificial que obteve melhor desempenho, com o objetivo de verificar a relevâncias das variáveis meteorológicas na estimativa da infestação de cigarrinha da cana-de-açúcar. Foi aplicado o teste do qui-quadrado para

verificar se a frequência dos dados observados difere da frequência dos dados esperados.

RESULTADOS E DISCUSSÃO

De acordo com a análise de componentes principais (PCA), as variáveis de maior importância na estimativa dos níveis de infestação de *Mahanarva fimbriolata* foram, umidade relativa, temperatura no ponto de orvalho, velocidade do vento média e temperatura máxima (Figura 2). Houve diferença estatística de acordo com o teste de qui-quadrado, portanto as variáveis meteorológicas influenciaram nos níveis de pressão populacional de *Mahanarva fimbriolata* na cana-de-açúcar.

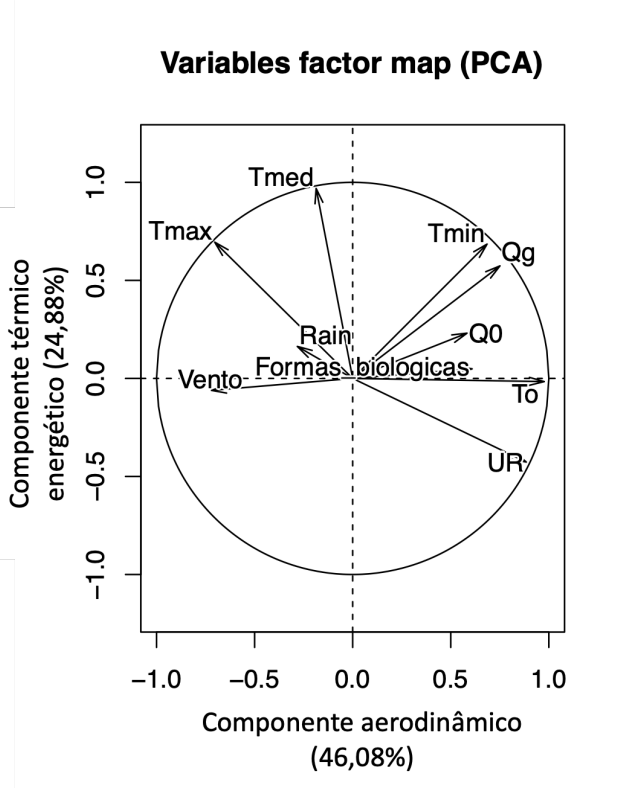

Figura 2. Análise dos componentes principais para os elementos climáticos utilizados na estimativa de formas biológicas de *Mahanarva fimbriolata* na cana-de-açúcar.

A ANS gerou quatros tipos de RNAs para estimarem a classificação da pressão populacional de cigarrinha na cana-de-açúcar (Tabela 1), duas Radial Basis Fuction (RBF), sendo a primeira com dez neurônios (RBF 10:10-10-3:1, dez variáveis de entrada, 10 neurônios na camada escondida, três classes de resposta e um neurônio

de saída) e outra com vinte e um neurônios (RBF 10:10-21-3:1), uma Multilayer Perception (MLP), com doze neurônios (6:6-12-3:1) e uma rede neural linear com três neurônios (Linear 8:8-3:1). Somente as redes RBF's utilizaram as 10 variáveis climatológicas.

Tabela 1. Estatística descritiva das Redes Neurais Artificiais geradas pelo Automatic Network Search na estimativa do número de formas biológicas de Mahanarva fimbriolata.

	MLP 6:6-12-3:1	RBF 10:10-10-3:1	Linear 8:8-3:1	RBF 10:10-21-3:1
Média (Formas Biológicas ha^{-1})	3344,93	3366,51	3372,02	3330,65
Desvio Padrão (Formas Biológicas ha^{-1})	1892,27	1911,02	2059,55	1955,87
Erro médio (Formas Biológicas $ha^{-1)}$	1689,43	2183,39	2101,15	1376,94
Correlação	0,57	0,60	0,60	0,61

Os valores médios de formas biológicas por hectare de *Mahanarva fimbriolata*, estimados pelas RNA's foram semelhantes, sendo que a maior média foi estimada pela rede Linear 8:8-3:1 com um valor de 3372,02 formas biológicas^{-1}, seguida pela RBF 10:10-10-3:1, 3366,51 formas biológicas^{-1}, MLP 6:6-12-3:1, 3344,93 formas biológicas^{-1} e por ultimo a que apresentou menor média a RBF com vinte e um neurônios, 3330,65 formas biológicas^{-1}. Quando ao erro médio das redes, o menor valor foi obtido pela RBF 10:10-21-3:1 de vinte e um neurônios, 1376,94 formas biológicas ha^{-1}. Entretanto a diferença do menor erro para o maior, 2183,39 formas biológicas ha^{-1}, que foi obtido pela RBF 10:10-10-3:1, foi de apenas 806 formas biológicas ha^{-1}, valor este menor que o desvio padrão médio das redes estudadas. A maior correlação e coeficiente de determinação também foram obtidos pela rede RBF de vinte e um neurônios, 0,61 e 0,37 respectivamente.

A comparação dinâmica dos dados estimados e observados confirma que a RNA conseguiu simular o comportamento da infestação de *Mahanarva fimbriolata*,

entretanto os picos observados, classificados como nível de pressão populacional alto, não foram capturados pela RNA (Figura 3).

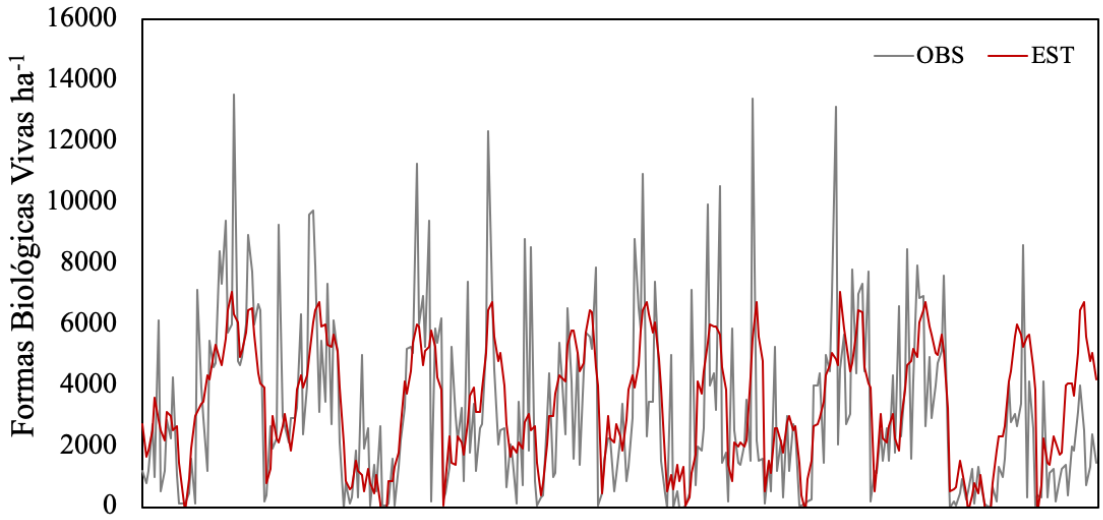

Figura 3. Resultados da comparação entre observado (cinza) e estimado (vermelho), pela rede neural artificial RBF 10:10-21-3:1.

Os níveis de infestação de *Mahanarva fimbriolata* foram classificados em pressões de população baixa, média e alta, de acordo com a distribuição da frequência dos dados coletados em campo (Tabela 2). Os resultados do desempenho das RNA's em classificar os níveis de pressão de população confirmaram os obtidos na estimativa das formas biológicas, em que o melhor desempenho foi o da RBF 10:10-21-3:1.

Este resultado corrobora com o obtido por Raad et al. (2012), onde os autores testaram as redes MLP e RBF para classificar tumores de câncer de mama, e a rede RBF foi mais eficiente do que a MLP. De acordo com Yilmaz and Kaynar (2011), as duas estruturas (MLP e RBF), são eficientes em resolver problemas de classificação, pois são robustas e com capacidade de generalizar dados de entrada imprecisos. Estes autores também verificaram uma melhor eficiência da RBF em relação a MLP.

Tabela 2. Desempenho das Redes Neurais Artificiais geradas pelo Automatic Network Search na estimativa da classificação da pressão populacional de Mahanarva fimbriolata.

	MLP 6:6-12-3:1			RBF 10:10-10-3:1			Linear 8:8-3:1			RBF 10:10-21-3:1		
	Baixo	Médio	Alto	Baixo	Médio	Alto	Baixo	Médio	Alto	Baixo	Médio	Alto
Total	204	104	7	204	104	7	204	104	7	204	104	7
Número de Acertos	174	44	0	179	55	0	178	49	0	176	59	0
Número de Erros	30	60	7	25	49	7	26	55	7	28	45	7
Correto (%)	85	42	0	88	53	0	87	47	0	86	57	0
Errado (%)	15	58	100	12	47	100	13	53	100	14	43	100

As MPL's já foram amplamente aplicadas em áreas distintas, executando tarefas como problemas de ajuste de função e reconhecimento de padrões, usando o treinamento supervisionado com um algoritmo conhecido como "Error Back Propagation" (Santos et al., 2013). Nas MPL's os neurônios estão dispostos em camadas, contando a partir da camada de entrada, que são os inputs (variáveis climáticas), depois vem as camadas ocultas e finalmente a camada de saída. As interligações só são permitidas entre duas camadas vizinhas. A rede é um avanço, isto é, os sinais de processamento se propagam da entrada para a saída (Zanaty, 2012).

Enquanto as MLP's apresentam várias camadas contendo uma variedade de funções de ativação e um complexo padrão de conectividade que contribuem para o valor de saída, as redes neurais RBF's são simples possuindo apenas três camadas: uma camada de entrada, uma camada escondida e uma camada de saída. De acordo com Santos et al. (2013) as redes RBF's além de um design fácil, apresentam boa generalização e alta tolerância aos ruídos de entrada (Santos et al., 2013).

A diferença em geral entre elas é que a RBF é um tipo de localista que é sensível somente a uma seção limitada de entrada espaço. Por outro lado, a MLP é uma abordagem mais distribuída (Yilmaz e Kaynar, 2011). O erro final atingido por uma RBF é menor que o de uma rede neural MLP e a convergência de uma RBF pode chegar a uma ordem de grandeza mais rápida do que a convergência de uma MLP; entretanto a capacidade de generalização da MLP é, em geral, superior a capacidade de generalização da RBF.

A rede RBF 10:10-21-3:1 obteve 86% de acertos na classificação de “Baixo”, 57% de acerto na classificação de “Médio” e 0% de acertos para a classificação “Alto”. Nenhuma das redes conseguiu classificar acuradamente a pressão populacional “Alto”, ou seja, a rede não consegue quantificar os picos populacionais (Figura 4). Uma das possíveis causa para esta limitação é o fato de que, a classificação por uma rede neural faz suposições sobre as classes e uma das principais pressuposições tipicamente feita é que o conjunto de classes foram definidas de forma exaustiva, caso isso não tenha ocorrido, certamente a acurácia da rede vai ser prejudicada (Foody, 2004).

Em termos práticos, entretanto, este resultado não minimiza a importância dos resultados, uma vez que, o nível de controle para *Mahanarva fimbriolata* não deve acontecer quando a pressão populacional for alta e sim antes. Somando as três classes, a rede acertou 235, de um total de 315, o que corresponde a um desempenho de aproximadamente 75%, o que comprova que as redes neurais artificiais são uma ferramenta viável para a determinação do nível de infestação de pragas.

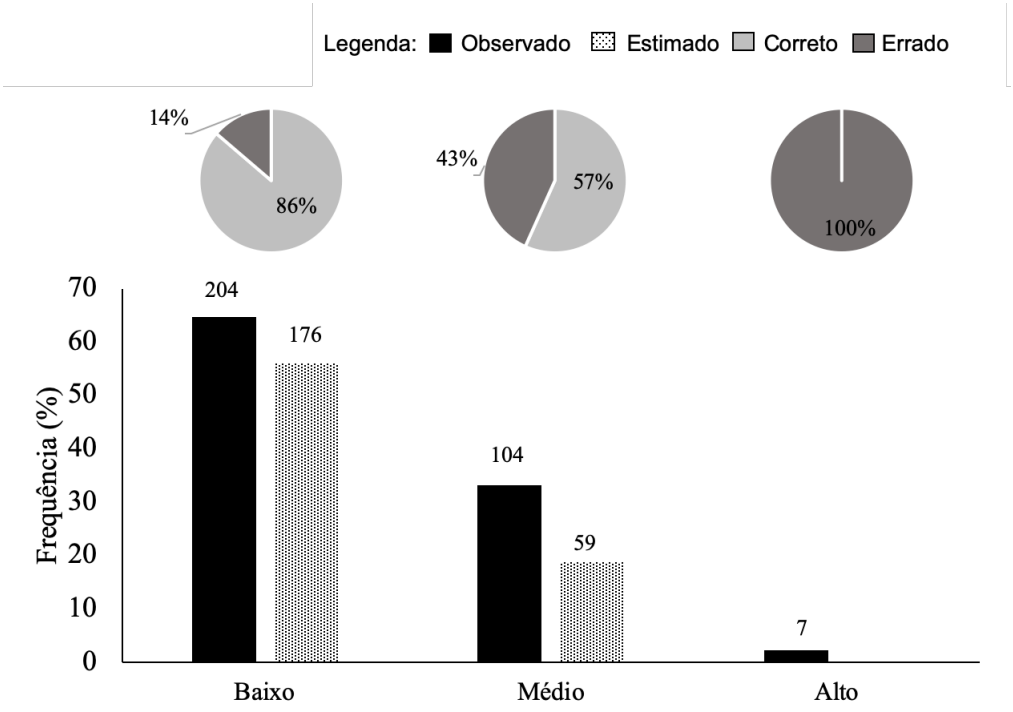

Figura 4. Resultados da comparação entre estimado e observado. Os histogramas referem-se a porcentagem da frequência dos dados observados e estimados pela

rede neural artificial RBF 10:10-21-3:1, enquanto que os gráficos de pizza reportam a porcentagem de acertos e erros.

CONLUSÕES

Um dos custos mais elevados nas áreas agrícolas é o tratamento fitossanitário. A técnica de redes neurais se mostrou uma ferramenta viável na estimativa dos níveis de pressão populacional de Mahanarva fimbriolata na cultura da cana-de-açúcar. Essa ferramenta permite a tomada de decisão de entrada ou não de pessoal e equipamentos no campo em função dessas estimações.

Diversas metodologias baseadas nas estruturas das redes podem ser replicadas, como Multilayer Perception, Radial Basis Fuction e até mesmo por uma rede Linear. A rede Radial Basis Fuction com três camadas sendo a primeira com 10 neurônios, a segunda com 21 e a terceira com 3 neurônios, foi a que obteve um melhor desempenho neste estudo. Estudos para aprimorar as técnicas de machine learning como as redes neurais na estimativa de infestações de pragas ainda são necessárias, principalmente quando a pressão populacional é alta.

REFERÊNCIAS

Azevedo MA, Andrade Júnior VCA, Sousa Júnior AS, Santos AS, Cruz CD, Pereira S L, Oliveira AJM (2017) Eficiência da estimação da área foliar de couve por meio de redes neurais artificiais. **Horticultura Brasileira**, 35: 014-019.

Binoti DHB, Binoti MLMS, Leite HG (2014) Configuração de redes neurais artificiais para a estimação do volume de árvores. **Ciência da Madeira**, 5(1): 58-67.

Bregaglio S, Donatelli M (2015) A set of software components for the simulation of plant airborne diseases. **Environ. Model. Softw.** 72: 426–444.

Chakraborty S, Ghos R, Ghosh M, Fernandes CD, Charchar MJ (2004) Weather-based prediction of anthracnose severity using artificial neural network models. **Plant pathol.** 53: 375-386.

Chakraborty S, Newton AC (2001) Climate change, plant diseases and food security: an overview. **Plant Pathol.** 60: 2-14.

Coakley SM, Scherm H, Chakraborty S (1999) Climate change and plant disease management. **Annu. Rev. Phytopathol.** 37: 399-426.

Dinardo-Miranda LL (2014) **Nematoides e pragas da cana-de-açúcar**. Campinas: Instituto Agronômico.

Dinardo-Miranda LL, Ferreira JMG, Carvalho PAM (2001) Influência da época de colheita e do genótipo de cana-de-açúcar sobre a infestação de *Mahanarva fimbriolata* (Stal) (Hemíptera: Cercopidae). **Neotropical Entomology**, 30(1): 145-149.

Donatelli M, Magarey RD, Bregaglio S, Willocquer L, Whish JPM, Savary S (2017) Modelling the impacts of pests and diseases on agricultural systems, **Agricultural Systems**, 155:213-224.

FOOD AND AGRICULTURE ORGANIZATION OF THE UNITED NATIONS - FAO (2016). Production. Disponível em: http://faostat3.fao.org/home/E Acesso em: 20 de ago. 2016.

Foody GM (2004) Supervised image classification by MLP and RBF neural networks with and without an exhaustively defined set of classes**. Int. J. Remote Sensing**, 25(15): 3091-3104.

Gaudart J, GIUSIANO B, HUIART L (2004) Comparison of the performance of multi-layer perceptron and linear regression for epidemiological data. **Neural Comput. Appl.**, 24: 47-70.

Gillespie TJ, Sentelhas PC (2008) Agrometeorology and plant disease management: a happy marriage. **Scientia Agricola**, 65: 71-75.

Laxmi RR, Kumar A (2011) Forecasting of powdery mildew in mustard (*Brassica juncea*) crop using artificial neural networks approach. **Indian J. Agric. Sci**, 81:855-860.

Magarey RC, Neilsen WA, Magnanini AJ (2004) Environmental requirements for spore germination in the three sugarcane leaf pathogens. In: Conference of the Australasian Society of Sugar Cane Technologists held at Brisbane, Queensland, 1-7.

Newman JA, Gibson DJ, Parsons AJ, Thornley, JHM (2003) How predictable are aphid population responses to elevated CO2. **J. Anim. Ecol**., 52: 556–566.

Pereira AR, Angelocci LR, Sentelhas PC (2002) Agrometeorology: Fundamentals and practical applications. Agropecuária, Guaíba.

Raad A, Kalakech A, Ayache M (2012) Brast cancer classification using neural network approach: MLP and RBF. The 13th International Arab Conference on Information Technology ACIT'2012 Dec.10-13

Santos RB, Rupp M, Bonzi SJ, Fileti AM (2013) Comparison Between Multilayer Feedforward Neural Networks and a Radial Basis Function Network to Detect and Locate Leaks in Pipelines Transporting Gas. **Chemical Engineering Transactions**, 32:1375-1380.

Savary S, Teng PS, Willocquet L, Nutter JRFW (2006) Quantification and modeling of crop losses: a review of purposes. **Annu. Rev. Phytopathol.** 44: 89–112.

Stackhouse P (2010) Prediction of worldwide energy resource. NASA Langley Research Center. https://power.larc.nasa.gov/ (accessed 13 Aug. 2018).

Vennila S, Singh G, Jha GK, Rao MS, Panwar H, Hegde M (2017) Artificial neural network techniques for predicting severity of *Spodoptera litura* (Fabricius) on groundnut. **Journal of Environmental Biology**, 38:1-8.

Whish JPM, Herrmann NI, White NA, Moore AD, Kriticos DJ (2015) Integrating pest population models with biophysical crop models to better represent the farming system. Environ. **Model. Softw.** 72: 418–425.

Yang X, Ming L, Chunjiang Z, Zheng Z, Yanlin H (2007) Early warning model for cucumber downy mildew in unheated greenhouses, **New Zealand Journal of Agricultural Research**, 50(5):1261-1268.

Yilmaz I, Kaynar O (2011) Multiple regression, ANN (RBF, MLP) and ANFIS models for prediction of swell potential of clayey soils. **Experts Systems with Applications**, 38: 5958-5966.

Zanaty EA (2012) Support Vector Machines (SVMs) versus Multilayer Perception (MLP) in data classification. **Egyptian Informatics Journal**,13(3): 177-183.

CAPÍTULO 4 - EVAPO: A smartphone application to estimate potential evapotranspiration using cloud gridded meteorological data from NASA-POWER system

ABSTRACT: In this study a new android app for smartphones to estimate potential evapotranspuration (ET_0) in real time, using gridded data from NASA-POWER, to any location in the world, would result in more efficient irrigation and increase irrigation water conservation. The smartphone app called EVAPO uses meteorological data to calculate ET_0 using the Penman–Monteith (FAO56) method. To evaluate performance of the proposed method, we compared ET_0 estimated by the EVAPO with that estimated from climatic data from conventional surface meteorological stations. The accuracy, tendency and precision of the models were determined using the Willmott et al. (1985) concordance index (d), systematic root mean square error (RMSEs) and correlation index (r^2), respectively. The results obtained were satisfactory for all studied locations whit mean values of 0.67, 0.95 (mm) and 0.72 for d, RMSEs and R^2, respectively.

KEYWORDS: internet of things; big data; irrigation; rational use of water.

EVAPO: Um aplicativo para smartphone para estimar a evapotranspiração potencial utilizando dados meteorológicos em grid do sistema NASA-POWER system

RESUMO: Neste estudo, foi desenvolvido um novo aplicativo de smartphones para estimar a evapotranspiração potencial (ET_0) em tempo real, utilizando dados em grid da NASA-POWER, para qualquer local do mundo, proporcionando uma irrigação mais eficiente e podendo aumentar a conservação do uso da água de irrigação. O aplicativo de smartphone chamado EVAPO utiliza dados meteorológicos para calcular ET_0 pelo método Penman-Monteith (FAO56). Para avaliar o desempenho do método proposto, comparamos o ET_0 estimado pelo EVAPO com o estimado a partir de dados climáticos de estações meteorológicas de superfície convencionais. A acurácia, tendência e precisão dos modelos foram determinadas utilizando o modelo de Willmott et al. (1985) índice de concordância (d), erro médio quadrático sistemático (RMSEs) e índice de correlação (r^2), respectivamente. Os resultados obtidos foram satisfatórios para todos os locais estudados, com valores médios de 0,67, 0,95 (mm) e 0,72 para d, RMSEs e r^2, respectivamente.

PALAVRAS-CHAVE: internet das coisas, big data, irrigação, uso racional da água.

INTRODUCTION

Agriculture is by far the largest water-use sector, accounting for about 70 percent of all water withdrawn worldwide from rivers and aquifers for crop production, domestic and industrial purposes (Siebert et al., 2013). Total area equipped for irrigation at the global scale is 307.6 million ha (Faoaquastat, 2016). Brazil is among the ten countries with the largest irrigated area in the world, with 6.95 million ha. The leaders are China and India, with about 70 million ha (Ana, 2017).

In several developing countries, irrigation represents up to 95% of all water withdrawn, and it plays a major role in food production and food security (Siebert et al., 2013). In Brazil, 67.2% of this water is destined for irrigation, with an annual average of 969 m^3s^{-1} (Ana, 2017). The use of water in an uncontrolled way can compromise the water resource (Silva et al., 2016). The agriculture development strategies depend on the possibility of maintaining, improving and expanding irrigated agriculture. In the last decade, the international community has made large efforts to assess the different elements of the water balance and to make irrigation management more precise (Sibert et a., 2013).

Evapotranspiration is an important parameter for climatological and hydrological studies as well as for agricultural water resources management, including irrigation planning and management (Allen et al., 2011; Lima et al., 2013; Djman et al., 2016). Many empirical methods have been developed over the last 50 years to estimate evapotranspiration (ET_0) from different climatic variables. Several studies around the world have concluded that the FAO-56 Penman-Monteith (FAO-PM) model is the most accurate one under different climatic conditions (Allen et al., 1998). FAO-PM have been tested in many regions in the world, including São Paulo (Brazil) (Camargo and Camargo, 2000), Florida (US) (Irmak et al., 2003), California (US) (Hargreaves and Allen, 2003), Bolivian Highlands (Bolivia) (Garcia et al., 2004), Reston (US) (ASCE, 2005), Albacete (Spain) (Lopez-Urrea et al., 2006), Hollabrunn (Austria) (Bodner et al., 2007), Florida (US) (Irmak et al., 2008), (Tunisian) (Jabloun and Sahli, 2008), Fredericton (Canada) (Xing et al., 2008), Western Balkans (Croatia and Serbia) (Trajkovic and Kolakovic, 2009), Florida (US) (Martinez and Thepadia, 2010), Crete

(Greece) (Xystrakis and Matzarakis, 2011), Southeast Australian (Azhar and Perera, 2011) and Rasht (Iran) (Tabari et al., 2013).

A more efficient irrigation, aimed at reducing the volumes of water applied and therefore increasing the conservation of irrigation water is possible by means of a real-time irrigation app smartphone throughout the territory (Migliaccio et al., 2015). One of the great advantages of using smartphones app is because they are examples of portable and easy-to-use technology, making it possible to facilitate decision-making in a real time basis (Delgado et al., 2012).

Agricultural researchers and extension specialists are using apps for a variety of uses, ranging from pest identification to irrigation scheduling (Vellidis et al., 2016). Some smartphones apps were developed, such as Vellidis et al. (2016), for irrigation scheduling in cotton and Migliaccio et al. (2015), who development a smartphone app for evaluation the performance of urban turf irrigation. However, in the literature no studies have been found that have made a smartphone app to aid in the irrigation of any culture and in any location around the world.

The major limitation of developing a work such as this on a large scale is the climate data inputs, which mostly come from automatic surface stations (Ramirez-Villegas and Challinor, 2012; Van Bussel et al., 2015; Monteiro et al., 2017). The use of gridded data (GD), is one method to solve this problem. Gridded data such as NASA-POWER's are systems that combine information from a variety of sources, e.g. surfaces, oceans and remote sensing. The objective of this work was to develop a smartphone app that estimates ET_0 in real time, making use of NASA-POWER's gridded data, to any location in the world.

MATERIAL AND METHODS

Agrometeorological data

The data series (Table 1), were downloaded from NASA-POWER (Stackhouse et al., 2017) https://power.larc.nasa.gov/.The NASA-POWER system was developed to provide meteorological information for direct use for architecture, power generation

and agrometeorology. It compiles information from various data sources directly and those derived from GDs. For example, real-time daily data for air temperature and relative humidity are obtained from the system of the Global Model and Assimilation Office (GEOS-4) and precipitation data are obtained from the Global Precipitation Climate Project. The grid used has a spatial resolution of 1 × 1°, which is equivalent to an area of approximately 12 347 km^2 (111.12 × 111.12 km) at the equator.

Table 1. Agrometeorological data from NASA-POWER, used for estimating the Evapotranspiration (ET_0) with Penman-monteith (FAO 56) method.

Agrometeorological data	**Description**	**Unit**
Q0	Daily Top-of-atmosphere Insolation	MJ m^{-2} day^{-1}
Qg	Daily Insolation Incident on a horizontal surface	MJ m^{-2} day^{-1}
Tmean	Average air temperature at 2 m above the surface of the Earth	ºC
Tmin	Minimum air temperature at 2 m above the surface of the Earth	ºC
Tmax	Maximum air temperature at 2 m above the surface of the Earth	ºC
RH	Relative Humidity at 2 m	%

Rain	Average precipitation	mm day^{-1}
Wind	Wind speed at 2 m above the surface of the Earth	m s^{-1}

* toa_dnw (Q0) and swn_dwn (Qg) is the name used by NASA.

Evapotranspiration (ET_0)

The model uses meteorological data to calculate ET0 using the Penman–Monteith equation (Eq. 1) (Allen et al., 1998). This method, also known as FAO 56, is widely accepted for irrigation scheduling, and its equation is given below:

$$ET_0 = \frac{0.408\,\Delta(Rn-G)+\gamma\frac{900}{Tmean+273}u_2(es-ea)}{\Delta+\gamma(1+0.34\,u_2)} \quad (1)$$

where ET0 is the reference evapotranspiration, in mm day^{-1}; Rn is the net radiation at the crop surface, MJ m^{-2} d^{-1}; G is the soil heat flux density, 0.8 MJ m^{-2} d^{-1}; T is the mean daily air temperature at 2 m , °C; u2 is the wind speed at 2 m, m s^{-1}; es is the saturation vapor pressure, kPa; ea is the actual vapor pressure, kPa; es-ea is the saturation vapor pressure deficit, kPa; Δ is the slope of the vapor pressure curve, kPa ºC^{-1}; γ is the psychrometric constant, 0.063 kPa °C^{-1}.

The slope of the vapor pressure curve, saturation vapor pressure and actual vapor pressure are calculated according to equations 2, 3 and 4.

$$\Delta = \frac{4098\left[0.6108\,exp\left(\frac{17.27\,Tmean}{Tmean+237.3}\right)\right]}{(Tmean+237.3)^2} \quad (2)$$

$$es = \frac{e_{Tmax}+e_{Tmin}}{2} \quad (3)$$

$$e_{Tmax} = 0.6108\,exp\left[\frac{17.27\,Tmax}{Tmax+237.3}\right] \quad (3.1)$$

$$e_{Tmin} = 0.6108\ exp\left[\frac{17.27\ Tmin}{Tmin+237.3}\right] \quad (3.2)$$

$$ea = e_{Tmin}\left[\frac{RH_{max}}{100}\right] \quad (3.3)$$

where, Tmax is the maximum daily air temperature, °C; Tmin is the minimum daily air temperature, °C; RHmax is the maximum relative humidity, %.

For the estimation of net radiation at the crop surface, we used the methodology proposed by An et al. (2017).

$$Rn = (1-\alpha)\ Qg - \left[ac\ \left(\frac{Qg}{Q0}\right) + bc\right]\left(a_1 + b_1 e_d^{0.5}\right)\sigma\ \left(\frac{Tmean^4+Tmin^4}{2}\right) \quad (5)$$

where, σ is the Stefan-Boltzmann Constant (5.67 x 10^{-8}); Tm is the mean temperature, °C; Tn is the minimum temperature, °C; ac and bc are the cloud factors, equal to 1.35 and -0.35, respectively; a_1 and b_1 are the emissivity factors, equal to 0.35 and -0.14, respectively, as suggested by Evett et al. (2011); α is the soil surface albedo (0.2); Qg is the Insolation Incident on a horizontal surface, Wm^{-2}; Q0 is the Top-of-atmosphere Insolation adjusted, Wm^{-2}, Eq. 6; e_d is the saturation vapor pressure.

$$Q0_{\ adjusted} = (0.75 + 0.00002\ EL_{msl})Q0 \quad (6)$$

where, EL_{msl} is the elevation (m) above the mean sea level.

Smartphone app development

Our design principles for the EVAPO were that it should provide the most accurate, site-specific, real-time information we could offer the user. In addition, the EVAPO would require minimum user input, just the coordinates of the location. Finally, the EVAPO would provide ready-to-use output.

The smartphone app was developed for devices with the Android operational system, written in Java programming language with help of the Android Studio 3.0 SDK (Software Development Kit), provided as an open source tool by Google and JetBrains. For the asynchronous HTTP requests made to get the data for the calculations, the

Volley library was used (Google Inc., 2017). Other libraries are used in the app, such as MPAndroidChart (Jahoda, 2018) and Android Sliding Up Panel (Umano, 2018).

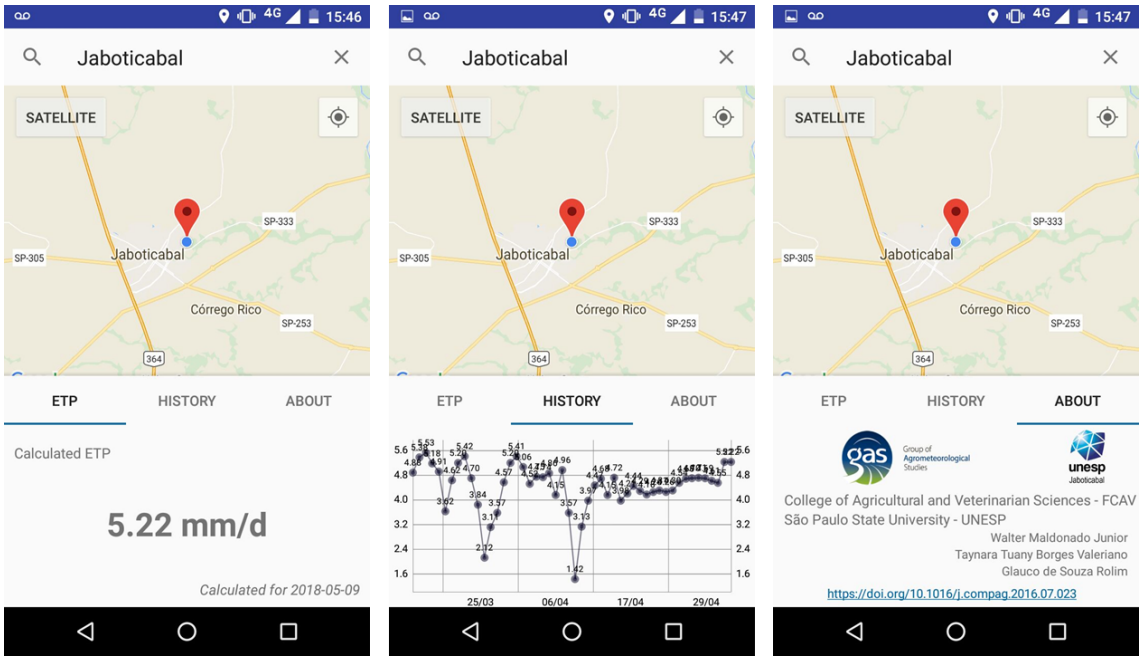

Figure 1. A complete workflow of the app. From left to right: ETP view, historic view, about view.

Performance analyses

To evaluate performance of the proposed method, we compared ET_0 estimated by the EVAPO with that estimated from climatic data from conventional surface stations at various locations worldwide (Table 2). The agrometeorological data used from conventional surface stations were mean, maximum and minimum air temperature at 2 m above the surface of the Earth (°C), relative humidity at 2 m (%), sunshine (hour) and wind speed (m s^{-1}).

Table 2. Coordinates, Altitude, Elevation and Source of the studied sites.

Location	Latitude	Longitude	Elevation	Source	Climate[1]
Porto de Moz, Brazil	01° 44′ 52″ S	52° 14′ 16″ W	15 m	INMET	Am
Jaboticabal, Brazil	21° 14′ 05″ S	48° 17′ 09″ W	615 m	FCAV/UNESP	Aw
Citra, United States	29° 24′ 42″ N	82° 06′ 36″ W	18.28 m	UF/FAWN	Cfa

Dublin, Ireland	53° 20′ 49″ N	06° 15′ 33″ W	71 m	Met Éireann	Cfb
Aachen, Germany	50° 46′ 00″ N	06° 06′ 00″ E	266 m	DWD	Cfb
Abucay, Philippines	14° 43′ 48″ N	120° 31′ 48″E	87 m	BSWN	Am

[1] Following the Köppen and Geiger climatic classification (1939). Legend: INMET, National Institute of Meteorology; FCAV/UNESP, São Paulo State University (Unesp), School of Agricultural and Veterinarian Sciences, Jaboticabal; UF/FAWN, University of Florida, Florida Automated Weather Network; Met Èireann, The Irish Meteorological Service; DWD, Deutsher Wetterdienst Climate Center. BSWN, Bureau of Soils and Water Management Department of Agriculture.

The ET0 estimated from surface data also used the methodology of FAO 56 (Eq. 1). However, we used the methodology proposed by Brunt (1934) (Eq. 7), for the estimation of net radiation. Global radiation (Qg) was estimated according Angström – Prescott (Eqs. 8 and 9) and Top-of-atmosphere Radiation (Q0) was estimated as described by Iqbal (1983).

$$Rn = [Qg(1-r)] + \left\{-\left[4.903\ x\ 10^{-9}\ Tmean^4\ \left(x_1 - x_2\ \sqrt{ea}\right)\ \left(0.1 + 0.9\ \frac{n}{N}\right)\right]\right\} \quad (7)$$

$$Qg = Q_0\ \left[a + b\ \frac{n}{N}\right] \quad (8)$$

$$a = 0.29 \cos ø \quad (9)$$

$$Q_0 = 37.6\ DR\ [(\pi/180) hn\ sen ø\ sen\delta + cos ø\ cos\delta\ sen\ hn] \quad (10)$$

$$DR = 1 + 0.033 \cos(360\ NDA/365) \quad (11)$$

$$hn = arcos[-tang\ ø\ tang\ \delta] \quad (12)$$

$$\delta = 23.45\ sen[(360/365)(NDA - 80)] \quad (13)$$

where, r is the coefficient of surface reflection, 0.20; T is mean temperature, K; x_1 and x_2 are equals to 0.56 and 0.25; ea is the actual vapor pressure, kPa; n is the sunshine, h; N is the photoperiod, h; a and b (0.52) are atmospheric attenuation

constant; ∅ is the latitude, degrees; DR is the distance relative earth sun; hn is the sunrise time, h; δ is the solar declination, degrees; NDA is the number of the day.

The performances of the ET_0 derived from conventional surface stations and NASA-POWER were assessed by linear regression analysis. The accuracy, tendency and precision of the models were determined using the Willmott et al. (1985) concordance index (d), systematic root mean square error (RMSEs) and correlation index (r^2), respectively.

$$d = 1 - \frac{\sum_{i=1}^{N} (Yobs_i - Yest_i)^2}{\sum_{i=1}^{N} (|Yest_i - \bar{Y}est| + |Yobs_i - \bar{Y}est|)} \quad (14)$$

$$RMSEs = \sqrt{\frac{\sum_{i=1}^{N} (Yobs_i - Yest_c)^2}{N}} \quad (15)$$

$$R^2 = \frac{\sum_{i=1}^{N} (Yest - \bar{Y}est)^2}{\sum_{i=1}^{N} (Yobs - \bar{Y}est)^2} \quad (16)$$

RESULTS AND DISCUSSION

We evaluated the performance of the models by comparing the ET_0 estimated using conventional surface stations data and gridded data, which represents EVAPO. The results obtained were satisfactory for all studied locations, which agrees with the authors who evaluated the application of the data in grid in several cases and concluded that gridded data of NASA-POWER can be used, generating precise and accurate results (Bai et al., 2010; Moeletsi and Walker, 2012; Bandaru et al., 2017; Monteiro et al., 2017; Battisti et al., 2018).

The average accuracy was 0.67 and minimum d was 0.44 for Dublin. All other locations presented values of d higher than 0.50, with a maximum of 0.88 in Aachen.

These results were similar to that found by Monteiro et al. (2017), in which was assessed how robust is the NASA/POWER database through its comparison with the Brazilian ground weather stations, where it was obtained an average d value of 0.57 for the ET_0.

Among the conditioning factors that may justify the variability of these data is the topography, changes in the land use or localized effects, that can be sources of errors in the models of data assimilation in the grid (White et al., 2008). According to Monteiro et al. (2017), even NASA-POWER offering a relatively coarse grid size database, some regional data fitting would give better results at higher latitudes and elevation.

All the locations presented a tendency, nevertheless very low values of RMSEs were found, with the maximum of 1.69 mm in Abucay. The minimum RMSEs was 0.31 mm in Porto de Moz and the mean value was 0.95 mm. Except for Porto de Moz, all the studied locations slightly overestimated the ET0 with the data of surface stations. Monteiro et al. (2017) also founded a tendency overestimating the surface data.

The reason for this tendency in all the studied locations may be attributed partially to the difference resolutions of the observations (Kishore et al. 2016), since the gridded data of NASA present a grid of 1 ° x 1 °. Another relevant factor is the inability to evaluate the performance of the surface data. Analyses of limited sets of stations have indicated that station-to-station errors can be as large as the GD errors (Wu et al., 2005; Mahmood et al., 2006; White et al., 2008). Both data sources have inherent errors and uncertainties in an equivalent matter.

The precision of the locations was similar, with R^2 ranging from 0.60 to 0.85. It was observed a relationship between the obtained precision and the climatic classification of the studied locations. The values of R^2 were smaller in locals where the climate is classified as Am and Aw, according to the methodology proposed by Köppen and Geiger (1939), being 0.60 for Porto de Moz, 0.60 for Jaboticabal and 0.65 for Abucay. The highest values of R^2 were obtained in the Cfa and Cfb climate, for Citra (0.83), Dublin (0.84) and Aachen (0.85).

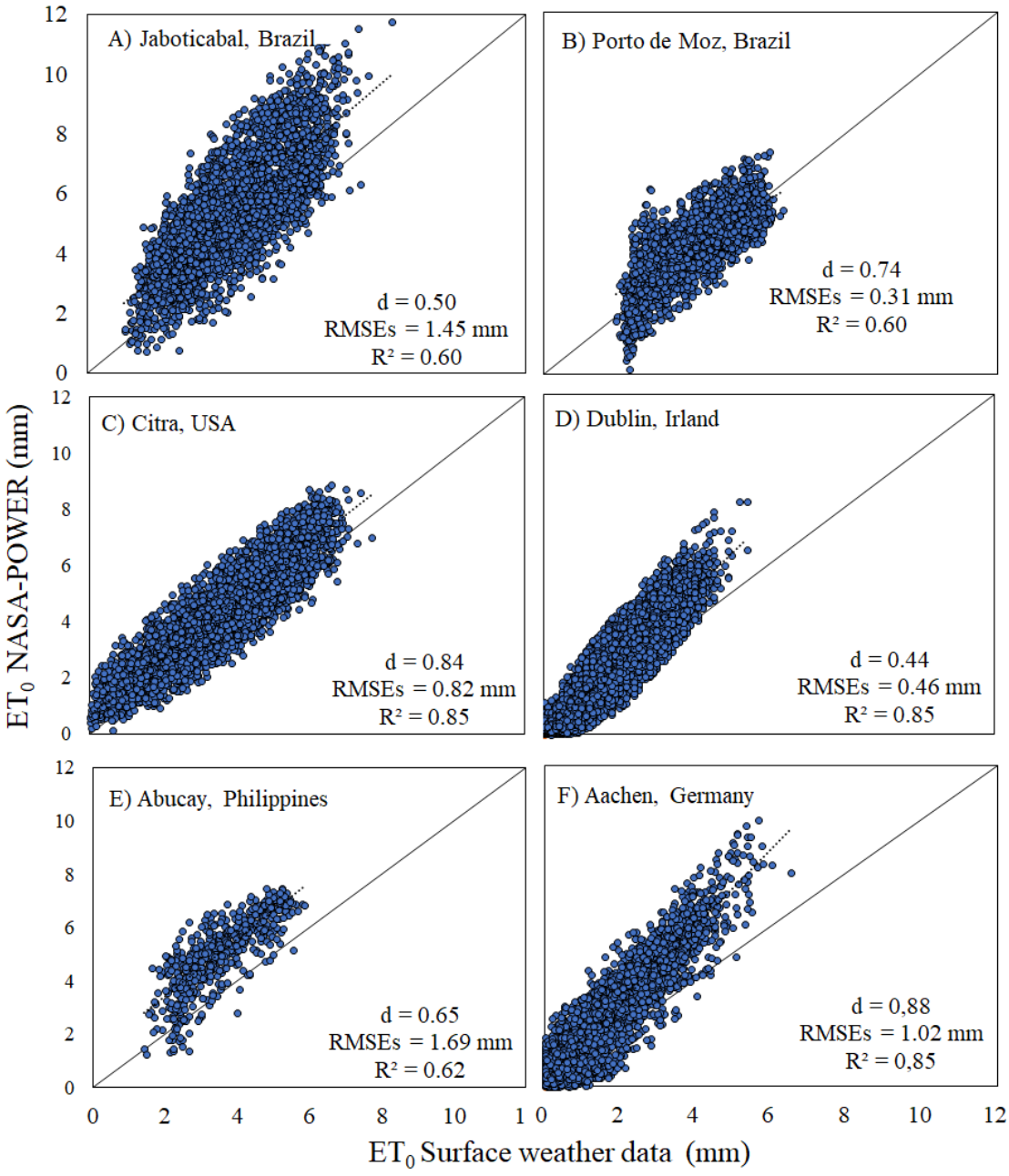

Figure 2. Relationship between ET_0 estimated by automatic surface stations and ET_0 estimated by NASA-POWER. Concordance index (d), systematic root means square error (RMSEs) and correlation index (r^2) are presented in the graphs. The black line is 1:1 line.

CONLUSIONS

EVAPO is a smartphone app developed for android smartphones for real-time estimation of the ET_0 (Potential Evapotranspiration) worldwide using climate gridded data from NASA-POWER. The results presented in this study allowed to conclude that NASA/POWER's gridded data can be used to estimate ET_0 reliably, enabling the applicability of the smartphone app.

REFERENCES

Agência Nacional de Águas (Brasil) – Conjuntura dos recursos hídricos no Brasil 2017: relatório pleno. Brasília, ANA, 265 p.

Allen RG, Pereira LS, Howell TA, Jensen ME (2011) Evapotranspiration information reporting: II. Recommended documentation. **Agric. Water Manage.**, 98(6), 921–929. https://doi.org/10.1016/j.agwat.2010.12.016.

Allen RG, Pereira LS, Raes D, Smith M (1998) Crop Evapotranspiration— Guidelines for Computing Crop Water Requirements. FAO Irrigation and Drainage Paper 56. Food and Agriculture Organization of the United Nations, Rome, Italy, ISBN 92-5-104219-5.

An N, Hemmati S, Cui Yu-Jun (2017) Assessment of the methods for determining net radiation at different time-scales of meteorological variables. **Journal of Rock Mechanics and Geotechnical Engineering**, 9 (2), 239 – 246. https://doi.org/10.1016/j.jrmge.2016.10.004.

ASCE-EWRI. (2005) **The ASCE standardized reference evapotranspiration equation**. Reston, VA.

Azhar AH, Perera BJC (2011) Evaluation of reference evapotranspiration estimation methods under Southeast Australian conditions. **J. Irrig. Drain Eng**., 268–279. https://ascelibrary.org/doi/10.1061/%28ASCE%29IR.1943-4774.0000297.

Bai J, Chen X, Dobermman A, Yang H, Cassman KG, Zhang F (2010) Evaluation of NASA satellite- and model-derived weather data for simulation of maize yield potential in **China. Agronomy Journal** 102 (1): 9–16. https://doi.org/10.2134/agronj2009.0085

Bandaru V, Pei Y, Hart Q, Jenkins BM (2017) Impact of biases in gridded weather datasets on biomass estimates of short rotation woody cropping systems. **Agric Forest Meteorol** 233:71–79. https://doi.org/10.1016/j.agrformet.2016.11.008

Battisti R, Bender FD, Sentelhas PC (2018) Assessment of different gridded weather data for soybean yield simulations in Brazil. **Theoretical and Applied Climatology**, 1-11. https://doi.org/10.1007/s00704-018-2383-y

Bodner G, Loiskandl W, Kaulm H (2007) Cover crop evapotranspiration under semi-arid conditions using FAO dual crop coefficient method with water stress compensation. **Agric. Water Manage.**, 93(3): 85–98. https://doi.org/10.1016/j.agwat.2007.06.010.

BSWM (2018), bureau of Soils and Water Management; Agro-meteorological Station. Available in: http://agromet.da.gov.ph/. (accessed 02.06.18).

Camargo ÂP, Camargo MBP (2000) An analytic revision of the potential evapotranspiration. **Bragantia**, 59(2): 125-137. http://dx.doi.org/10.1590/S0006-87052000000200002

Delgado JA, Kowalski K, Tebbe C (2012) The first Nitrogen Index app for mobile devices: Using portable technology for smart agricultural management. **Computers and Eletronics in Agriculture**, 91: 121-123. http://dx.doi.org/10.1016/j.compag.2012.12.008.

Djaman K, Irmak S, ASCE M, Kabenge I, Futakuchu K (2016) Evaluation of FAO-56 Penman-Monteith model with limited data and the valiantzas models for estimating grass-reference evapotranspiration in Sahelian Conditions. J**ournal of Irrigation and Drainage Engineering**, 04016044: 1-14.

DWD Climate Data Center (CDC): Historical daily station observations (temperature, pressure, precipitation, sunshine duration, etc.) for Germany, version v005, 2017.

Evett SR, Prueger JH, Tolk JA (2011) Water and energy balances in the soil-plant atmosphere continuum. In: Huang PM, Li Y, Sumner ME, editors. Handbook of soil sciences: properties and processes. 2nd ed. Boca Raton, Florida, USA: CRC Press; 6-1-6-44.

FAO. 2016. AQUASTAT website. Food and Agriculture Organization of the United Nations (FAO). Website accessed on [2018/01/22].

Garcia M, Raes D, Allen R, Herbas C (2004) Dynamics of reference evapotranspiration in the Bolivian highlands (Altiplano). **Agric. Forest Meteorol.,** 125(1–2): 67–82. https://doi.org/10.1016/j.agrformet.2004.03.005.

Google Inc., 2017. Recursos do Android Studio | Android Studio [WWW Document]. URL https://developer.android.com/studio/features.html (accessed 11.16.17).

Hargreaves GH, Allen RG (2003) History and evaluation of Hargreaves evapotranspiration equation. **J. Irrig. Drain. Eng.**, 1(53): 53–63. http://dx.doi.org/10.1061/(ASCE)0733-9437(2003)129:1(53).

INMET (2018), Instituto Nacional de Meteorologia, Banco de Dados Meteorológicos para Ensino e Pesquisa. Disponível em: http://www.inmet.gov.br/portal/index.php?r=bdmep/bdmep (accessed 02.06.18).

IQBAL M (1983) **An Introduction to Solar Radiation**. New York: Academic Press, 390 p.

Irmak S, Irmak A, Jones JW (2003). Solar and net radiationbased equations to estimate reference evapotranspiration in humid climates. **J. Irrig. Drain. Eng.**, 129:5(336): 336–347. http://dx.doi.org/10.1061/(ASCE)0733-9437(2003)129:5(336).

Irmak S, Irmak A, Howell TA, Martin DL, Payero JO, Copeland KS (2008) Variability analyses of alfalfa-reference to grass-reference evapotranspiration ratios in growing and dormant seasons. **J. Irrig. Drain. Eng**., 134:2(147): 147–159. http://dx.doi.org/10.1061/(ASCE)0733-9437(2008)134:2(147).

Jabloun M, Sahli A (2008) Evaluation of FAO-56 methodology for estimating reference evapotranspiration using limited climatic data application to Tunisia. **Agrc. Water Manage.**, 95(6): 707–715. https://doi.org/10.1016/j.agwat.2008.01.009.

Jahoda P (2018) MPAndroidChart. https://github.com/PhilJay/MPAndroidChart.

L´opez-Urrea R, Martín de Santa Olalla F, Fabeiro C, Moratalla A (2006) Testing evapotranspiration equations using lysimeter observations in a semiarid climate. **Agric. Water Manage.**, 85(1–2): 15–26. https://doi.org/10.1016/j.agwat.2006.03.014.

Lima J, Antonino A, Souza E, Hammecker C, Montenegro S, Lira C (2013) Calibration of Hargreaves-Samani equation for estimating reference evapotranspiration in sub-humid region of Brazil. **J. Water Resour. Prot**., 5(12A): 1–5. http://dx.doi.org/10.4236/jwarp.2013.512A001

Martinez CJ, Thepadia M (2010) Estimating reference evapotranspiration with minimum data in Florida, USA. **J. Irrig. Drain. Eng.**, 494–501. http://dx.doi.org/10.1061/(ASCE)IR.1943-4774.0000214.

METéireann (2018), The Irish Meteorological Service Online. Available in: http://www.met.ie/. (accessed 02.06.18).

Migliaccio KW, Morgan KT, Fraisse C, Vellidis G, Zotarelli L, Fraisse C, Zurweller BA, Andreis JH, Crane JH, Rowland D (2015) Smartphone apps for irrigation scheduling. Trans. ASABE 59 (1): 291–301. http://dx.doi.org/10.13031/trans.59.11158.

Monteiro LA, Sentelhas PC, Pedra GU (2017) Assessment of NASA/POWER satellite-based weather system for Brazilian conditions and its impact on sugarcane yield simulation. **Int. J. Climatol**. 38(3): 1571-1581. https://doi.org/10.1002/joc.5282

Siebert S, Henrich V, Frenken K, Burke J (2013) Update of the Global Map of Irrigation Areas to version 5. Project report, 178 p.

Silva ECR, Alves FB, Silva IIS (2016) Irrigated agriculture in the Amazon context: A systematic approach to the use of water in a horticulture in the municipality of Atamira-PA. **Revista Internacional de Ciências**, 6 (1): 29 – 43.

Stackhouse Jr PW, Westberg D, Chandler WS, Zhang T, Hoell JM (2017) Prediction of Worldwide Energy Resource (POWER) Agroclimatology Methodology, version 1.1.0, may 30. NASA Langley Research Center. Available on https://power.larc.nasa.gov/.

Tabari H, Grismer M, Trajkovic S (2013) Comparative analysis of 31 reference evapotranspiration methods under humid conditions. **Irrig. Sci.**, 31(2): 107–117. http://dx.doi.org/10.1007/s00271-011-0295-z.

Taghadomi-Saberi S, Omid M, Emam-Djomeh Z, Ahmadi H (2013) Development of an intelligent system to determine sour cherry's antioxidant activity and anthocyanin content during ripening. **Int. J. Food Prop**. 17: 1169–1181. https://doi.org/10.1080/10942912.2012.702182.

Trajkovic S, Kolakovic S (2009) Evaluation of reference evapotranspiration equations under humid conditions. **Water Resour. Manage.**, 23(14): 3057–3067. https://doi.org/10.1007/s11269-009-9423-4.

UF/FAWN (2018), University of Florida, Florida Automated Weather Network. Available in: https://fawn.ifas.ufl.edu/data/. (accessed 02.06.18).

Umano: News read to you (2018) Android Sliding Up Panel. https://github.com/umano/AndroidSlidingUpPanel.

Vellidis G, Liakos V, Andreis J, Perry C, Porter W, Barnes E, Morgan K, Fraisse C, Migliaccio K (2016) Development and assessment of smartphone application for irrigation scheduling in cotton. **Com. Electron. Agric.** 127: 249-259. https://doi.org/10.1016/j.compag.2016.06.021.

Xing Z, Chow L, Meng F, Rees HW, Monteith J, Lionel S (2008) Testing reference evapotranspiration estimation methods using evaporation pan and modeling in maritime region of Canada. **J. Irrig. Drain. Eng**., 417–424. http://dx.doi.org/10.1061/(ASCE)0733-9437(2008)134:4(417).

Xystrakis F, Matzarakis A (2011) Evaluation of 13 empirical reference potential evapotranspiration equations on the island of Crete in southern Greece. **J. Irrig. Drain Eng.**, 211–222. http://dx.doi.org/10.1061/(ASCE)IR.1943-4774.000028